Trend Analysis and Time-Series Forecasting of Climate Variability in Urban and Rural Settlements of Niger State, Nigeria

Yisa Jacob[1]; Jiya Solomon Ndace[2]; Abubakar Danjuma Sheikh[3]; Abdullahi Ibrahim[4]

[1]Department of Geography, Faculty of Physical Science, Ibrahim Badamasi Babangida University, Lapai, Nigeria.

[2]Department of Geography, Faculty of Physical Science, Ibrahim Badamasi Babangida University, Niger State, Nigeria.

[3]Department of Geography, Faculty of Physical Science, Ibrahim Badamasi Babangida University, Niger State, Nigeria.

[4]Department of Computer Science, Faculty of Physical Science, Ibrahim Badamasi Babangida University, Niger State, Nigeria

DOI: https://doi.org/10.47772/IJRISS.2026.100700316

Received: 15 July 2026; Accepted: 20 July 2026; Published: 31 July 2026

ABSTRACT

Climate variability has become a major environmental concern due to its implications for water resources, agriculture, ecosystem sustainability, and human livelihoods. This study analysed historical climate trends and forecasted future climate variability in selected urban and rural settlements of Niger State, Nigeria, using statistical and time-series techniques. Annual rainfall and temperature data covering the period 1994–2024 were analysed using the Mann–Kendall trend test and Sen's Slope estimator, while future climate conditions were projected using Autoregressive Integrated Moving Average (ARIMA) models. The results revealed significant warming trends across the study area. Temperature increased by approximately 16.0°C in Mokwa and Muwo, 18.2°C in Minna and Garatu, 17.1°C in Kontagora, and 2.9°C in Rafin Gora between 1994 and 2024. Rainfall exhibited spatial variability, with substantial declines in some settlements and slight increases in others. Mann–Kendall and Sen's Slope analyses confirmed increasing temperature trends and varying rainfall patterns. The ARIMA model identification process indicated that ARIMA(1,2,1) was suitable for rainfall forecasting, while ARIMA(1,1,1) adequately modelled temperature variations. Diagnostic statistics confirmed the adequacy of the selected models, with non-significant Ljung–Box statistics indicating white-noise residuals.

Forecasts suggest continued temperature increases and increasing climate variability across both urban and rural settlements up to 2054. The study concludes that climate variability in Niger State is intensifying and may pose significant environmental and socio-economic challenges if adaptation measures are not implemented. The study recommends the integration of climate forecasting into regional planning, strengthening of climate monitoring systems, and implementation of adaptation strategies to enhance resilience.

Keywords: Climate variability, trend analysis, Rainfall Trends; Temperature Trends; ARIMA, Mann–Kendall, Sen's Slope, rainfall forecasting, temperature forecasting.

INTRODUCTION

Climate variability has emerged as one of the most critical environmental issues affecting societies across the globe. Fluctuations in climatic parameters, particularly temperature and rainfall, exert considerable influence on water resources, agricultural productivity, biodiversity conservation, and socio-economic progress (IPCC, 2023). Over the last few decades, many parts of the world have witnessed rising temperatures, changing precipitation patterns, and an increasing occurrence of extreme weather events, thereby intensifying concerns regarding environmental sustainability and human welfare.

The African continent is especially susceptible to the impacts of climate variability because of its heavy reliance on climate-dependent sectors, notably agriculture and water resources (Niang et al., 2014). Across West Africa, climatic conditions have undergone substantial changes during recent decades, marked by increasing temperatures and considerable fluctuations in rainfall regimes (Sylla et al., 2016). These climatic disturbances have significant implications for food security, ecosystem resilience, and overall economic development within the region.

Nigeria has also experienced considerable variations in its climatic conditions. Empirical studies have documented increasing temperature trends and inconsistent rainfall patterns across the country's various ecological zones (Ayanlade et al., 2018; Oguntunde et al., 2020). Such climatic alterations present serious challenges to agricultural production, water resource management, and environmental sustainability, thereby increasing the vulnerability of both human and natural systems.

Situated within the Guinea Savannah ecological zone, Niger State occupies an important position in Nigeria's agricultural landscape and contributes significantly to national food production. Nevertheless, increasing climatic variability poses growing threats to agricultural activities, ecosystem services, and socio-economic development within the state. Despite the growing need for reliable climate information to support adaptation planning and sustainable resource management, comprehensive investigations of climate variability across both urban and rural settlements in Niger State remain inadequate. Consequently, this study focuses on analysing historical climatic trends and forecasting future climate variability in selected urban and rural settlements of Niger State over the period 1994–2054.

LITERATURE REVIEW

The Concept of Climate

Climate can be described as the long-term average condition and statistical representation of atmospheric variables within a particular region, encompassing elements such as temperature, precipitation, humidity, wind characteristics, and atmospheric pressure over extended periods, usually spanning several decades or more (World Meteorological Organization [WMO], 2017; Intergovernmental Panel on Climate Change [IPCC], 2021). In contrast to weather, which reflects short-term atmospheric conditions at a specific location and time, climate represents the persistent patterns and variations that influence both natural ecosystems and human activities (IPCC, 2021). It incorporates not only average climatic conditions but also the variability and occurrence of extreme events, thereby providing an essential basis for understanding environmental continuity and change (WMO, 2017).

Climate is governed by complex interactions among various components of the Earth system, including the atmosphere, hydrosphere, cryosphere, lithosphere, and biosphere, which continuously exchange energy and matter across different temporal and spatial scales (IPCC, 2021; Trenberth et al., 2007). Consequently, climate should be viewed as a dynamic and interconnected system rather than a static environmental condition.

Furthermore, climatic conditions are strongly influenced by global energy balances and a range of external forcing mechanisms. Solar radiation serves as the principal source of energy driving atmospheric processes, and variations in solar output and orbital parameters, commonly referred to as Milankovitch cycles, contribute to long-term climatic fluctuations (IPCC, 2021). Major volcanic eruptions also affect climate by releasing aerosols into the stratosphere, thereby reducing incoming solar radiation and inducing temporary cooling effects. These external drivers interact with ocean–atmosphere systems such as the El Niño–Southern Oscillation (ENSO), generating climatic variability over different temporal scales (Trenberth et al., 2014). Contemporary climate science therefore conceptualizes climate as a complex and coupled system that evolves under the combined influence of natural processes and anthropogenic activities (IPCC, 2021). Within this framework, climate variability refers to fluctuations around long-term climatic averages, whereas climate change denotes persistent alterations in climatic characteristics over extended periods (IPCC, 2021). Understanding climate as a dynamic statistical system is essential for adaptation planning, vulnerability assessment, and the development of resilience strategies aimed at addressing environmental change (Field et al., 2014).

Climate Variability

Climate variability refers to temporal fluctuations in climatic elements, including temperature, rainfall, humidity, wind speed, and solar radiation occurring over monthly, annual, or decadal timescales. Unlike climate change, which generally denotes long-term alterations in climatic conditions largely associated with anthropogenic greenhouse gas emissions, climate variability encompasses both natural and human-induced departures from long-term climatic averages (Intergovernmental Panel on Climate Change [IPCC], 2023). Such fluctuations may arise from natural mechanisms such as atmospheric circulation changes, volcanic activity, and ocean–atmosphere interactions, as well as from anthropogenic influences including urbanisation, deforestation, and industrial development.

Among the various climatic elements, rainfall and temperature are particularly important indicators of climate variability because of their direct influence on agricultural production, water resources, ecosystem functioning, and human livelihoods. Variations in rainfall patterns determine the availability of water for domestic consumption, irrigation activities, and hydroelectric power generation, whereas temperature changes affect evapotranspiration rates, crop yields, biodiversity, and public health conditions (United Nations Environment Programme [UNEP], 2024). Consequently, the assessment of long-term trends in temperature and rainfall has become increasingly important in supporting climate adaptation measures and sustainable development initiatives.

Recent decades have witnessed a marked intensification of climate variability at the global scale. The IPCC (2022) reported that global average surface temperature has risen by approximately 1.1°C above pre-industrial levels, accompanied by an increase in the occurrence of heatwaves, prolonged droughts, and irregular precipitation regimes. The report further highlighted that many regions are increasingly experiencing extreme rainfall events, thereby elevating the risks of flooding and environmental degradation.

Africa remains one of the region’s most vulnerable to climatic fluctuations because of its substantial dependence on climate-sensitive sectors such as agriculture and water resources. According to the World Meteorological Organization (2024), the continent has experienced above-average temperatures over the past decade, while rainfall patterns have become increasingly unpredictable, resulting in recurrent drought episodes in some areas and severe flooding in others. These climatic disturbances have considerable implications for food security, ecosystem integrity, and socio-economic development.

Within West Africa, rainfall and temperature variability constitute major environmental concerns. Previous studies have documented substantial changes in precipitation regimes since the severe Sahelian droughts of the 1970s and 1980s (Nicholson, 2018). Although certain areas have shown signs of rainfall recovery, variability in precipitation remains a significant environmental and socio-economic challenge across the region.

Nigeria has likewise experienced considerable climatic fluctuations over recent decades, characterised by increasing temperatures and marked spatial differences in rainfall distribution. Using the Mann–Kendall trend test and Sen's Slope estimator, Iyeme et al. (2024) identified widespread warming trends across the country, while rainfall patterns displayed considerable regional variability, with some locations exhibiting increasing trends and others experiencing declining precipitation. Similar observations have been reported by recent studies, which suggest that urbanisation and land-use changes have intensified local climatic modifications through rising surface temperatures and altered rainfall patterns (Oyeniyi et al., 2025).

In the present study, climate variability is represented using annual rainfall and temperature records obtained from six selected settlements between 1994 and 2024. Historical climatic trends were examined using the Mann–Kendall trend test and Sen's Slope estimator, whereas future climatic conditions up to 2054 were projected using Autoregressive Integrated Moving Average (ARIMA) models. The integration of these statistical approaches provides a robust framework for understanding both past climatic behaviour and future climate variability within the study area.

Causes of Climate Variability

Climate variability results from the interaction of internal climate system dynamics and external forcing mechanisms (IPCC, 2021). One of the principal drivers of climatic fluctuations is the complex interaction between the atmosphere and oceans. Internal ocean–atmosphere processes play a significant role in regulating global climatic conditions through the redistribution of heat and moisture within the Earth system.

Among these processes, the El Niño–Southern Oscillation (ENSO) is particularly important. ENSO events are characterized by periodic warming (El Niño) and cooling (La Niña) of sea surface temperatures in the equatorial Pacific Ocean, leading to significant alterations in global rainfall and temperature patterns (IPCC, 2021). Likewise, the Atlantic Multidecadal Oscillation (AMO) contributes to multi-decadal variations in North Atlantic temperatures and has substantial implications for precipitation patterns in regions such as West Africa and North America (IPCC, 2021). The Pacific Decadal Oscillation (PDO) also influences long-term climatic conditions within the Pacific region and contributes to variations in drought occurrence and precipitation regimes (IPCC, 2023). These oscillatory processes occur naturally through feedback mechanisms involving the oceans, atmosphere, land surfaces, and cryosphere.

External natural forcing mechanisms also contribute significantly to climate variability. Volcanic eruptions, for instance, release large quantities of aerosols into the stratosphere, which reflect incoming solar radiation and temporarily reduce global temperatures (IPCC, 2021). Similarly, fluctuations in solar irradiance associated with periodic solar cycles influence the quantity of energy reaching the Earth's surface and contribute to natural climatic fluctuations (IPCC, 2021). Although the influence of solar variability has become relatively less significant compared with anthropogenic factors in recent decades, it remains an important component of natural climate variability.

In contemporary times, anthropogenic activities have become major contributors to both climate variability and long-term climatic change. Increasing concentrations of greenhouse gases, including carbon dioxide (CO_2), methane (CH_4), and nitrous oxide (N_2O), intensify the greenhouse effect and contribute to rising global temperatures and changes in precipitation patterns (IPCC, 2021). Furthermore, human-induced land-use modifications such as deforestation, agricultural expansion, and urbanisation alter surface albedo, evapotranspiration processes, and atmospheric composition, thereby influencing regional and local climatic conditions (IPCC, 2021). The interaction between these anthropogenic activities and natural climatic processes often amplifies climatic extremes and increases the variability of rainfall and temperature patterns in many regions of the world.

Effects of Climate Variability

Climate variability exerts substantial impacts on agricultural productivity and food security, particularly in regions where livelihoods depend predominantly on rain-fed agricultural systems (IPCC, 2022). Irregular rainfall patterns, including uncertain onset and cessation of rainy seasons, disrupt planting schedules and crop development processes, thereby increasing the risks of reduced yields and crop failure (FAO, 2023). Temperature variations further influence crop phenology by modifying growing seasons and affecting evapotranspiration rates and soil moisture conditions (IPCC, 2022). Rising temperatures also alter pest and disease dynamics, often leading to increased infestations and declining agricultural productivity (FAO, 2023). Consequently, many countries in Africa and Asia have experienced recurring food insecurity, unstable incomes, and heightened vulnerability among smallholder farming communities as a result of climatic fluctuations (IPCC, 2022).

Human health is also significantly affected by climate variability through increasing occurrences of heatwaves, cold events, and changes in the distribution of vector-borne diseases (WHO, 2023). Extreme heat conditions increase the incidence of heat-related illnesses, cardiovascular disorders, and mortality,

ISSN No. 2454-6186 | DOI: 10.47772/IJRISS | Volume X Issue VII July 2026

particularly among elderly populations and urban residents exposed to intensified thermal stress (IPCC, 2022). Changes in precipitation regimes can further alter the habitats and geographical distribution of disease vectors such as mosquitoes, thereby increasing the transmission of malaria, dengue fever, and other vector-borne diseases (WHO, 2023). In addition, fluctuations in rainfall patterns can adversely affect water quality and sanitation infrastructure, increasing the prevalence of water-borne diseases such as cholera and diarrhoeal infections (UNEP, 2024). These health challenges place considerable pressure on public health systems and impose significant socio-economic costs, especially in developing countries with limited adaptive capacities (IPCC, 2022).

Water resources represent one of the sectors most sensitive to climatic variability because changes in the amount, timing, and intensity of precipitation directly influence hydrological processes (IPCC, 2022). Variability in rainfall patterns affects river discharge, groundwater replenishment, and reservoir storage, thereby complicating water resource planning for domestic, agricultural, and industrial uses (UNESCO, 2024). Increased occurrences of droughts and extreme rainfall events can either reduce water availability or trigger flooding, both of which pose challenges to effective water management (IPCC, 2022). In coastal environments, variations in sea level and storm surges may lead to saltwater intrusion into freshwater aquifers, threatening the availability of safe drinking water (UNEP, 2024).

Ecosystems and biodiversity are equally vulnerable to climatic fluctuations because changes in temperature and moisture regimes influence species distribution, reproductive processes, and ecosystem productivity (Intergovernmental Science-Policy Platform on Biodiversity and Ecosystem Services [IPBES], 2023). Rapid and persistent climatic variations may exceed the adaptive capacities of many species, resulting in habitat degradation, biodiversity loss, and disruption of ecosystem services that are essential for human wellbeing (IPCC, 2022).

Numerous studies have highlighted the sensitivity of agriculture to variations in temperature and rainfall, particularly regarding their effects on crop yields and food security (Lobell et al., 2011; IPCC, 2022). Rain-fed agricultural systems in Africa and Asia are considered especially vulnerable because of their dependence on climatic conditions (Sultan & Gaetani, 2016). Likewise, human health is increasingly threatened by heat stress, rising mortality rates, and changing disease transmission dynamics (Haines & Ebi, 2019). Urban areas are particularly susceptible due to urban heat island effects, which intensify exposure to extreme temperatures and heatwaves (Oke, 1982; IPCC, 2022). Furthermore, water resources are highly responsive to variations in rainfall timing and intensity, affecting recharge processes and supply reliability (Vörösmarty et al., 2010). Ecosystems also respond to climatic fluctuations through modifications in species composition and ecosystem productivity, and in some cases, climatic changes may exceed ecological tolerance limits, resulting in irreversible environmental changes (Parmesan & Yohe, 2003).

Climate Variability (Trends) Detection

The Mann–Kendall (MK) trend test is widely recognised as one of the most reliable non-parametric methods for identifying monotonic trends in time-series data. Initially introduced by Mann (1945) and subsequently refined by Kendall (1975), the method employs a rank-based approach to determine whether a dataset exhibits an increasing or decreasing trend without requiring assumptions of normality, homoscedasticity, or linear relationships among variables. Owing to its ability to handle non-normal datasets, missing observations, and extreme values, the Mann–Kendall test has become a standard technique for analysing long-term environmental, hydrological, and climatic records (Helsel et al., 2020).

In contrast to parametric regression techniques, the Mann–Kendall procedure relies on the sequential ordering of observations rather than their absolute magnitudes. The test statistic (S) is obtained by comparing each observation in the time series with all subsequent observations. Positive values of S indicate an upward trend, whereas negative values signify a downward trend. For large sample sizes, the S statistic is transformed into a standardized Z statistic, which is then evaluated against the standard normal distribution to determine the significance of the detected trend. When the associated probability value (p-value) is lower than the selected significance threshold, usually 0.05, the null hypothesis of no trend is rejected, suggesting the presence of a statistically significant temporal trend (Mann, 1945; Kendall, 1975).

ISSN No. 2454-6186 | DOI: 10.47772/IJRISS | Volume X Issue VII July 2026

A major advantage of the Mann–Kendall test lies in its resistance to the effects of outliers and skewed data distributions. Climatic variables such as temperature and rainfall commonly exhibit irregular distributions, serial dependence, and occasional extreme events, conditions under which conventional parametric methods may produce unreliable results. Consequently, the Mann–Kendall test has gained widespread acceptance as an effective tool for assessing long-term climatic variability, hydrological alterations, and environmental change across different geographical regions (Gilbert, 1987; Helsel et al., 2020).

Although the Mann–Kendall test is effective in determining the existence and direction of trends, it does not provide information regarding the magnitude of change. To address this limitation, the test is frequently used together with the Sen's Slope estimator, which quantifies the rate of increase or decrease in a variable over time. The combined application of these two techniques enables researchers to evaluate both the statistical significance and the magnitude of climatic trends, thereby making them complementary approaches in hydro-meteorological investigations (Sen, 1968; Helsel et al., 2020).

The Sen's Slope estimator, developed by Pranab Kumar Sen, is likewise a non-parametric technique designed to estimate the magnitude of monotonic trends in time-series datasets (Sen, 1968). Unlike ordinary least squares regression, the method is relatively insensitive to extreme values and does not require assumptions of normality or variance homogeneity. The estimator computes the median of all possible pairwise slopes within a dataset, thereby providing a robust and reliable estimate of the rate of temporal change (Helsel et al., 2020).

Recent studies continue to demonstrate the applicability and effectiveness of the Mann–Kendall and Sen's Slope methods in climate research. Iyeme et al. (2024), for example, applied these techniques to long-term meteorological records across Nigeria and reported significant warming trends in several parts of the country. Their findings also revealed substantial spatial variations in rainfall, with certain locations exhibiting increasing trends while others experienced declining precipitation. The study concluded that the integration of the Mann–Kendall test and Sen's Slope estimator provides dependable evidence for evaluating climate variability in Nigeria.

Similarly, Şen (2024) introduced an enhanced moving trend analysis approach for hydro-meteorological time series and reaffirmed the importance of the Mann–Kendall test as a benchmark method for validating temporal changes in climatic variables. The study emphasized that non-parametric techniques are particularly valuable when climatic data exhibit irregular fluctuations, non-linearity, and complex temporal behaviour.

Despite recent advancements in machine learning and artificial intelligence applications in climate science, the Mann–Kendall test remains one of the most widely adopted and easily interpretable statistical approaches for trend detection. Its computational efficiency, minimal statistical assumptions, and robustness against outliers have ensured its continued relevance in climate change studies, hydrological investigations, environmental monitoring, and water-resource management (Helsel et al., 2020).

In the present study, the Mann–Kendall test was applied to evaluate long-term trends in rainfall and temperature between 1994 and 2024 within selected urban settlements (Mokwa, Minna, and Kontagora) and rural settlements (Muwo, Garatu, and Rafin Gora) in Niger State. The test was used to determine the existence and direction of significant monotonic trends in each climatic variable, while the corresponding Sen's Slope estimator was employed to quantify the rate of climatic change. The findings derived from these analyses provided the statistical basis for assessing historical climate variability and subsequently informed the ARIMA-based forecasting of future rainfall and temperature conditions.

Prediction of Climate Variability

Forecasting climate variability involves modelling the complex interactions among atmospheric, oceanic, and terrestrial systems over seasonal, interannual, and decadal timescales (IPPC, 2021). Contemporary climate prediction approaches increasingly adopt seamless forecasting frameworks that integrate seasonal and multi-annual simulations to improve the prediction of temperature and precipitation anomalies (Doblas-

Reyes et al., 2013; Merryfield et al., 2020). By constraining transient climate simulations using observed conditions and analogue techniques, these approaches often produce more reliable predictions than unconstrained ensemble simulations, thereby providing useful information for sectors such as agriculture, water resources management, and environmental planning (Smith et al., 2019).

Among the various statistical forecasting techniques, the Autoregressive Integrated Moving Average (ARIMA) model remains one of the most widely applied methods for analysing and predicting time-series data. Developed by George E. P. Box and Gwilym M. Jenkins, the ARIMA model integrates three fundamental components: autoregressive (AR), integrated (I), and moving average (MA) processes (Box et al., 2015). The model is commonly expressed as ARIMA (p, d, q), where p represents the autoregressive order, d denotes the level of differencing required to attain stationarity, and q indicates the order of the moving average component. The underlying assumption of the model is that future observations can be explained by previous observations and past forecast errors once the series has been transformed into a stationary process (Hyndman & Athanasopoulos, 2021).

The simplicity, flexibility, and strong predictive capability of the ARIMA model have contributed to its widespread application in climatology, hydrology, environmental sciences, economics, and numerous other disciplines (Agaj et al., 2024; Fan, 2025). According to Box and Jenkins (1976), the ARIMA modelling framework consists of four major stages: model identification, parameter estimation, diagnostic evaluation, and forecasting. These procedures continue to form the basis of modern time-series modelling and are incorporated into various statistical software packages, including SPSS, R, and Python.

Model selection and evaluation are typically based on several performance criteria, including the Akaike Information Criterion (AIC), Bayesian Information Criterion (BIC), Root Mean Square Error (RMSE), Mean Absolute Percentage Error (MAPE), and the Ljung–Box Q statistic. These indicators assist in determining the adequacy, goodness-of-fit, and forecasting performance of competing ARIMA specifications.

Recent empirical studies have further demonstrated the effectiveness of ARIMA models in climate-related forecasting applications. Agaj et al. (2024), for example, applied ARIMA techniques to forecast hydrological water levels and reported that the models generated reliable predictions suitable for sustainable environmental management and long-term planning. Their findings indicated that ARIMA effectively captured temporal dependencies within the datasets and produced stable forecasts with relatively low prediction errors.

Similarly, Fan (2025) conducted a comparative assessment of ARIMA and Exponential Smoothing (ETS) models using the NASA GISTEMP temperature anomaly dataset. The study revealed that ARIMA outperformed ETS models for long-term temperature forecasting based on lower AIC, BIC, and Mean Square Error (MSE) values, concluding that ARIMA provides greater predictive stability in situations where seasonal effects are relatively weak. Likewise, Elneel et al. (2024) utilised autoregressive models to predict global sea-level variations and concluded that ARIMA remains one of the most robust forecasting approaches for environmental datasets because of its ability to capture temporal dependence while maintaining a relatively simple parameter structure.

In climate variability research, ARIMA models are particularly useful because annual rainfall and temperature records frequently exhibit temporal dependence but limited seasonality after annual aggregation. Consequently, ARIMA provides dependable medium- and long-term forecasts that support planning and decision-making by improving understanding of future climatic conditions under changing environmental circumstances. For the present study, ARIMA (1,2,1) was selected for rainfall forecasting, whereas ARIMA (1,1,1) was adopted for temperature forecasting following comprehensive model evaluation using AIC, BIC, RMSE, MAPE, and Ljung–Box diagnostic statistics. These model specifications were considered appropriate because they adequately represented the temporal characteristics of the climatic variables and demonstrated satisfactory forecasting performance.

ISSN No. 2454-6186 | DOI: 10.47772/IJRISS | Volume X Issue VII July 2026

Research Gap

Despite the increasing volume of research on climate variability at global and national scales, several important knowledge gaps remain. Existing studies have largely focused on isolated assessments of rainfall variability, temperature trends, or climate change impacts, with relatively few investigations integrating these components within a single analytical framework capable of supporting future climate prediction. Although numerous studies on climate variability have been undertaken in different regions of Nigeria, limited attention has been given to the simultaneous examination of historical climate trends and future climatic projections across both urban and rural settlements in Niger State. Most previous investigations have either concentrated on specific locations or considered urban and rural environments separately, thereby limiting understanding of the spatial differences and similarities in climatic behaviour between these settlement types.

Furthermore, there remains a paucity of studies that combine trend analysis techniques with statistical forecasting approaches to provide comprehensive assessments of both historical and future climate variability within the state. Consequently, empirical evidence regarding long-term climatic behaviour across urban and rural contexts in Niger State remains inadequate. This study therefore addresses these deficiencies by integrating climate trend analysis and forecasting techniques to examine historical and future rainfall and temperature variability across selected urban and rural settlements in Niger State. The study contributes to existing knowledge by providing a comprehensive assessment of climate variability within diverse settlement contexts and generating empirical evidence that can support sustainable urban planning, environmental management, agricultural adaptation, and climate resilience strategies within the state.

MATERIALS AND METHODS

Study Area

Niger State is located in the central region of Nigeria and the largest state in the country by area, sharing borders with several states including Benin Republic in the West, Zamfara State (North), Kebbi (North West). Kwara (South West), Kaduna (North East) and the Federal Capital Territory (FCT) Abuja (South East). It is located between latitude $8^0$30'N to $11^0$30'N and between longitude $03^0$30'E to $07^0$30'E (National Bureau of Statistics, 2022). The study is carried out in three political zones (Niger South, Niger East and Niger West, that is, Zones A, B and C) of the state, which is specifically delimited within Niger State, encompassing six communities of urban and rural (Mokwa and Muwo in Zone A, Minna and Garatu in Zone B and Kontagora and Rafin Gora in Zone C). These locations were selected due to their varying levels of urbanization and spatial growth patterns, making them suitable for comparative analysis of urban sprawl.

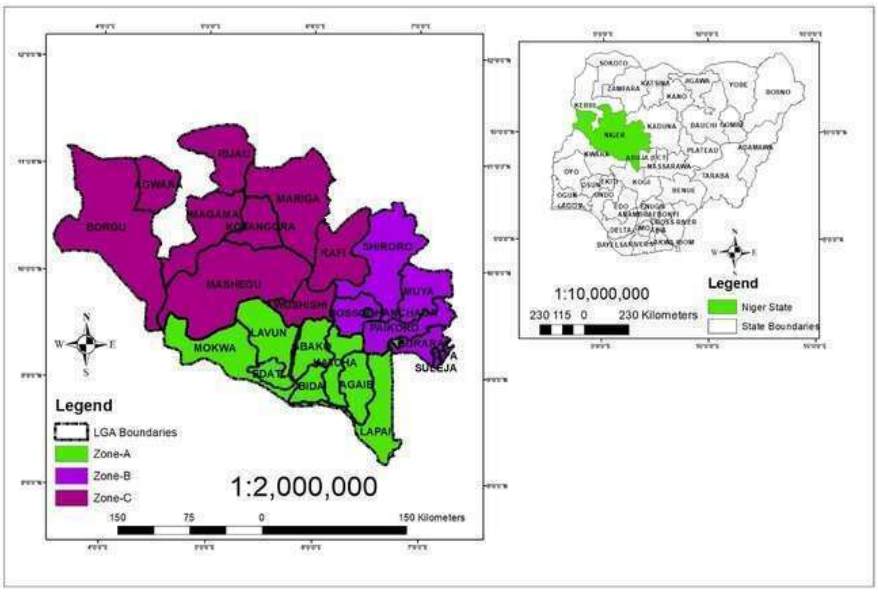

Figure 1: Map of Niger State showing Zones A, B and C

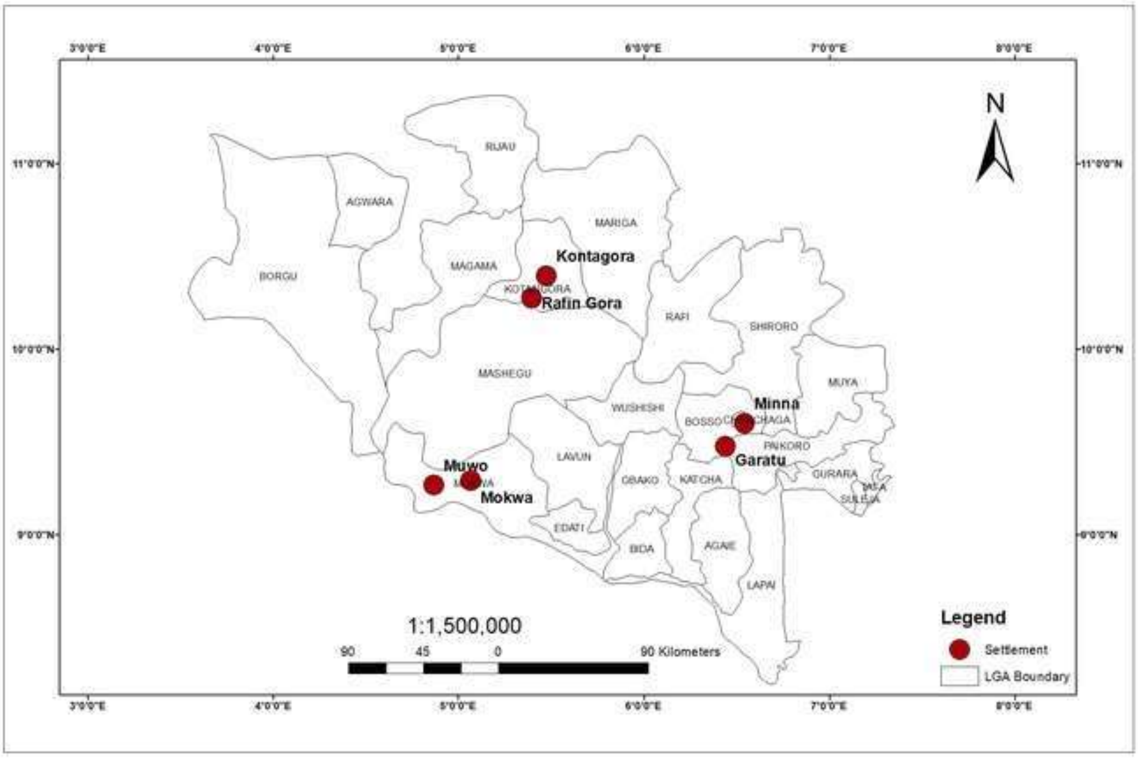

Figure 2: Map of Niger State showing the Selected Six Settlements

Data Sources

Temperature and rainfall data (1994–2024) were sourced from the National Aeronautics and Space Administration (NASA) Langley Research Centre's Prediction of Worldwide Energy Resources (POWER).

Data Analysis and Presentation

Mann-Kendall Trend Test

The Mann-Kendall test was applied to detect significant monotonic trends in rainfall and temperature data.

$$S = \sum_{i=1}^{n-1} \sum_{j=i+1}^{n} sign(X_j - X_i)$$

Where:

- X_j and X_i are observations
- n is the sample size

Sen's Slope Estimator

The magnitude of climate trends was estimated using Sen's Slope:

$$Q = \frac{X_j - X_i}{j - i}$$

The median of all pairwise slopes was selected as the trend estimate.

ISSN No. 2454-6186 | DOI: 10.47772/IJRISS | Volume X Issue VII July 2026

Time Series Analysis Using ARIMA Model

The Box–Jenkins Autoregressive Integrated Moving Average (ARIMA) modelling framework was adopted to analyse and forecast annual rainfall and temperature patterns in the selected settlements (Mokwa, Muwo, Minna, Garatu, Kontagora and Rafin Gora). The modelling process involved four principal stages, namely; stationarity assessment, model identification, parameter estimation and model selection, and diagnostic evaluation. Following the establishment of the most suitable models, future projections of rainfall and temperature were generated up to the year 2054.

Test for Stationarity (Augmented Dickey–Fuller Test)

Before fitting the ARIMA model, the rainfall and temperature series were tested for stationarity using the Augmented Dickey–Fuller (ADF) unit root test. A stationary time series has a constant mean and variance over time and is required for reliable ARIMA modelling.

The hypotheses tested during model stationarity were:

H_0: The time series contains a unit root (non-stationary).

H_1: The time series is stationary.

The decision rule adopted was:

I. Reject H_0 if $p < 0.05$

II. Fail to reject H_0 if $p > 0.05$

Where non-stationarity existed, first or second differencing was applied until stationarity was achieved.

Model Identification Using ACF and PACF

After stationarity was achieved, the Autocorrelation Function (ACF) and Partial Autocorrelation Function (PACF) plots were examined to determine appropriate autoregressive (AR) and moving average (MA) orders.

Model identification followed the Box–Jenkins procedure:

I. PACF cutoff → AR order (p)

II. ACF cutoff → MA order (q)

Parameter Estimation and Model Selection

Several competing ARIMA models were estimated.

The final model was selected using

I. Lowest AIC

II. Lowest BIC

III. Lowest RMSE

IV. Lowest MAPE

V. Highest Stationary R^2

ISSN No. 2454-6186 | DOI: 10.47772/IJRISS | Volume X Issue VII July 2026

VI. Significant AR and MA coefficients

Model Diagnostic Checking

The adequacy of the selected models was evaluated through residual analysis.

The following diagnostics were employed:

I. Residual ACF

II. Residual PACF

III. Ljung–Box Q Test

A model was considered adequate if:

I. residual autocorrelations were insignificant,

II. residual PACF values lay within the 95% confidence limits,

III. Ljung–Box p-value exceeded 0.05.

Validation and Reliability of the Instruments and Models

To validate ARIMA model, several ARIMA specifications were initially considered during model identification. Based on stationarity and diagnostic assessments, ARIMA(1,2,1) was adopted for rainfall forecasting, while ARIMA(1,1,1) was adopted for temperature forecasting. Model adequacy was evaluated using Akaike Information Criterion (AIC), Bayesian Information Criterion (BIC), Root Mean Square Error (RMSE), Mean Absolute Percentage Error (MAPE), and Ljung–Box Q statistics. These models demonstrated superior predictive performance and were subsequently applied consistently across all study locations.

RESULTS AND DISCUSSION

Magnitude of Climate Variability (Temperature and Rainfall Trends)

The climate variables/data (rainfall and temperature) collected from the study locations were subjected to time series analysis in order to show the trend of the data collected for the time frame of study (1994-2024). Trend analysis was conducted using the Mann–Kendall non-parametric test and Sen's Slope estimator to determine the direction and magnitude of rainfall and temperature trends between 1994 and 2024. Table 1 presents the results of the Mann–Kendall trend test and Sen's Slope Estimator across the six study settlements between 1994 and 2024. The Mann–Kendall statistics reveal varying rainfall trends across the study area, whereas temperature consistently exhibits positive trends.

Climate Variability/Trends

For Mokwa and Muwo, the results presented in Table 1 indicate that annual rainfall exhibited a declining tendency, as shown by the Mann–Kendall S statistic of −17, Z-value of −0.272, and Sen's Slope estimate of −0.94 mm/year. The negative Sen's Slope suggests a gradual reduction in rainfall during the study period, although the relatively low Z-value indicates that the declining trend is weak. In contrast, annual temperature demonstrated a marked upward trend, with an S statistic of 257, Z-value of 4.351, and Sen's Slope of +0.51°C per year. This positive slope signifies a sustained increase in temperature over time.

Similarly, Minna and Garatu also exhibited decreasing rainfall trends. The two settlements recorded Mann–Kendall S statistics of −48, corresponding Z-values of −0.770, and Sen's Slope estimates of −2.15 mm/year. These values suggest a stronger decline in rainfall relative to Mokwa and Muwo. Conversely, temperature

ISSN No. 2454-6186 | DOI: 10.47772/IJRISS | Volume X Issue VII July 2026

trends in both settlements were strongly positive, with S statistics of 269, Z-values of 4.560, and Sen's Slope estimates of +0.58°C per year. The relatively higher positive slope indicates that the rate of warming in Minna and Garatu is slightly greater than that observed in Mokwa and Muwo.

In contrast to other locations (Mokwa, Muwo, Minna, and Garatu), Kontagora and Rafin Gora experienced increasing rainfall trends throughout the study period. Both settlements recorded Mann–Kendall S statistics of 96, Z-values of 1.540, and Sen's Slope estimates of +4.32 mm/year, indicating progressive increases in annual rainfall. Temperature patterns, however, showed some variation between the two locations. Kontagora exhibited a pronounced warming trend, with an S statistic of 281, Z-value of 4.780, and Sen's Slope of +0.55°C per year. By comparison, Rafin Gora experienced a relatively weaker increase in temperature, as reflected by an S statistic of 108, Z-value of 1.820, and Sen's Slope estimate of +0.09°C per year. Nevertheless, both settlements demonstrated positive temperature trends over the study period.

Therefore, the results reveal considerable spatial variation in rainfall patterns across Niger State. Declining rainfall tendencies were observed in Mokwa, Muwo, Minna, and Garatu, whereas increasing rainfall trends characterised Kontagora and Rafin Gora. In contrast, temperature exhibited consistent upward trends across all settlements, indicating a widespread warming phenomenon irrespective of settlement type. These findings suggest that climate variability within the study area is more strongly characterised by persistent increases in temperature than by uniform changes in rainfall patterns.

Table 1: Analysis of Mann–Kendall and Sen's Slope Estimator Across Six Study Locations

Location	**Variable**	**MK S-Value**	**Z-value**	**Sen's Slope**	**Trend**
Mokwa	Rainfall	-17	-0.272	-0.94 mm/yr	Decreasing
Mokwa	Temperature	257	4.351	+0.51 °C/yr	Increasing
Muwo	Rainfall	-17	-0.272	-0.94 mm/yr	Decreasing
Muwo	Temperature	257	4.351	+0.51 °C/yr	Increasing
Minna	Rainfall	-48	-0.77	-2.15 mm/yr	Decreasing
Minna	Temperature	269	4.56	+0.58 °C/yr	Increasing
Garatu	Rainfall	-48	-0.77	-2.15 mm/yr	Decreasing
Garatu	Temperature	269	4.56	+0.58 °C/yr	Increasing
Kontagora	Rainfall	96	1.54	+4.32 mm/yr	Increasing
Kontagora	Temperature	281	4.78	+0.55 °C/yr	Increasing
Rafin Gora	Rainfall	96	1.54	+4.32 mm/yr	Increasing
Rafin Gora	Temperature	108	1.82	+0.09 °C/yr	Increasing

Source: Author’s Computation (2026)

Trend line graphs presented in Figures 3 to 14 shows the annual rainfall and temperature patterns across the study settlements between 1994 and 2024. Results from Figures 3 to 8 indicate that rainfall exhibited varying but generally weak long-term trends, accompanied by considerable interannual fluctuations across the six settlements of Mokwa, Muwo, Minna, Garatu, Kontagora, and Rafingora. Mokwa and Muwo displayed identical rainfall characteristics, with an average annual rainfall of approximately 1,027.6 mm. Both locations experienced only a marginal decline of about 0.256 mm per year, equivalent to an overall reduction of approximately 7.94 mm (0.77%) during the study period. The very low coefficient of determination ($R^2 = 0.0001$) indicates that time contributed negligibly to rainfall variation, suggesting an absence of a meaningful long-term rainfall trend.

ISSN No. 2454-6186 | DOI: 10.47772/IJRISS | Volume X Issue VII July 2026

Conversely, Minna and Garatu experienced more pronounced declines in rainfall. The trend analysis revealed annual decreases of approximately 13.59 mm, amounting to cumulative reductions of about 421 mm over the 31-year period. This represents overall decreases of approximately 34% and 28.9% for Minna and Garatu, respectively. However, the explanatory strength of the trend remained relatively weak, as indicated by an R^2 value of 0.1264. In contrast, Kontagora and Rafingora exhibited increasing rainfall tendencies, with annual increases of approximately 13 mm, resulting in cumulative gains of about 390 mm (29.3%) during the study period. Nevertheless, the low coefficient of determination ($R^2 = 0.0817$) suggests that the observed increase is relatively weak and largely masked by substantial year-to-year variability. Consequently, rainfall behaviour across the study area appears to be influenced more by cyclical and interannual climatic fluctuations than by persistent directional changes, indicating that regional atmospheric processes exert greater control on rainfall patterns than temporal progression alone. Temperature trends shown in Figures 9 to 14 exhibited a markedly different pattern, revealing strong and persistent warming across most of the settlements. Mokwa and Muwo recorded identical warming trends, with annual temperatures increasing at a rate of approximately 0.59°C per year. This corresponds to an overall increase of about 18.4°C over the study period, representing an increase of approximately 51% above the baseline mean temperature. The relatively high coefficient of determination ($R^2 = 0.692$) indicates that nearly 69% of the observed temperature variation can be explained by temporal changes.

Similarly, Minna and Garatu experienced even stronger warming trends, with annual temperature increases of approximately 0.62°C per year, amounting to cumulative increases of about 19.2°C (55%) during the study period. The corresponding R^2 values of 0.696 further confirm the persistence and significance of the warming trend in these locations. Among the urban settlements, Kontagora recorded the highest rate of warming, with temperatures increasing by approximately 0.64°C annually, resulting in an overall increase of about 19.8°C (57%). The coefficient of determination ($R^2 = 0.6072$) also indicates a strong positive relationship between temperature and time. In contrast, Rafin Gora exhibited only a weak warming signal, with temperatures increasing by approximately 0.02°C per year, equivalent to an overall increase of about 0.62°C (1.6%) during the study period. The very low R^2 value of 0.0076 suggests that annual temperature fluctuations were much more influential than any persistent long-term warming trend in the settlement, despite its relatively high mean temperature.

The trend analysis therefore, demonstrates that temperature is undergoing a consistent and substantial long-term increase across Niger State, whereas rainfall remains largely characterised by considerable interannual variability and weak or inconsistent long-term trends. The most pronounced warming trends were observed in the rapidly urbanising centres of Minna, Mokwa, and Kontagora. This pattern may be associated with increasing urban expansion, the proliferation of impervious surfaces, loss of vegetation cover, anthropogenic heat emissions, and the intensification of urban heat island effects. The rural settlements generally exhibited temperature patterns similar to those of their adjacent urban centres, implying that regional climatic change, land degradation, and peri-urban land-use transformations are extending warming effects beyond urban boundaries.

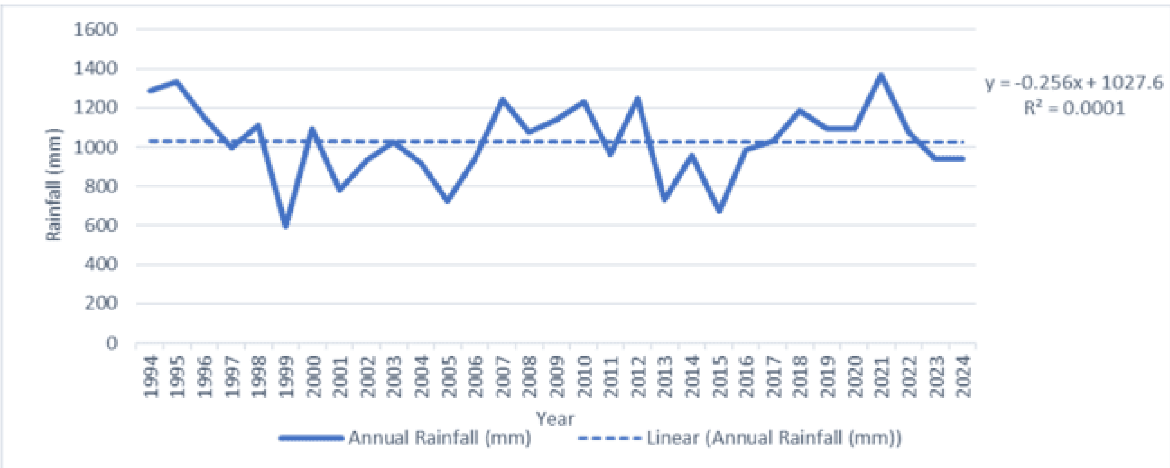

Figure 3: Mokwa Rainfall Trend (1994–2024)

ISSN No. 2454-6186 | DOI: 10.47772/IJRISS | Volume X Issue VII July 2026

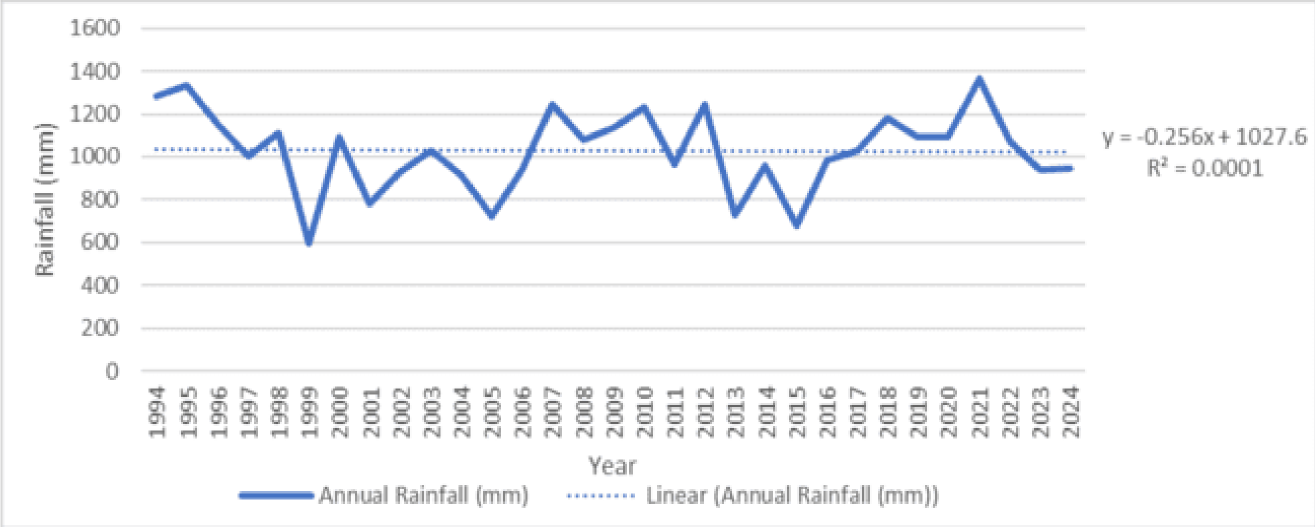

Figure 4: Muwo Rainfall Trend (1994–2024)

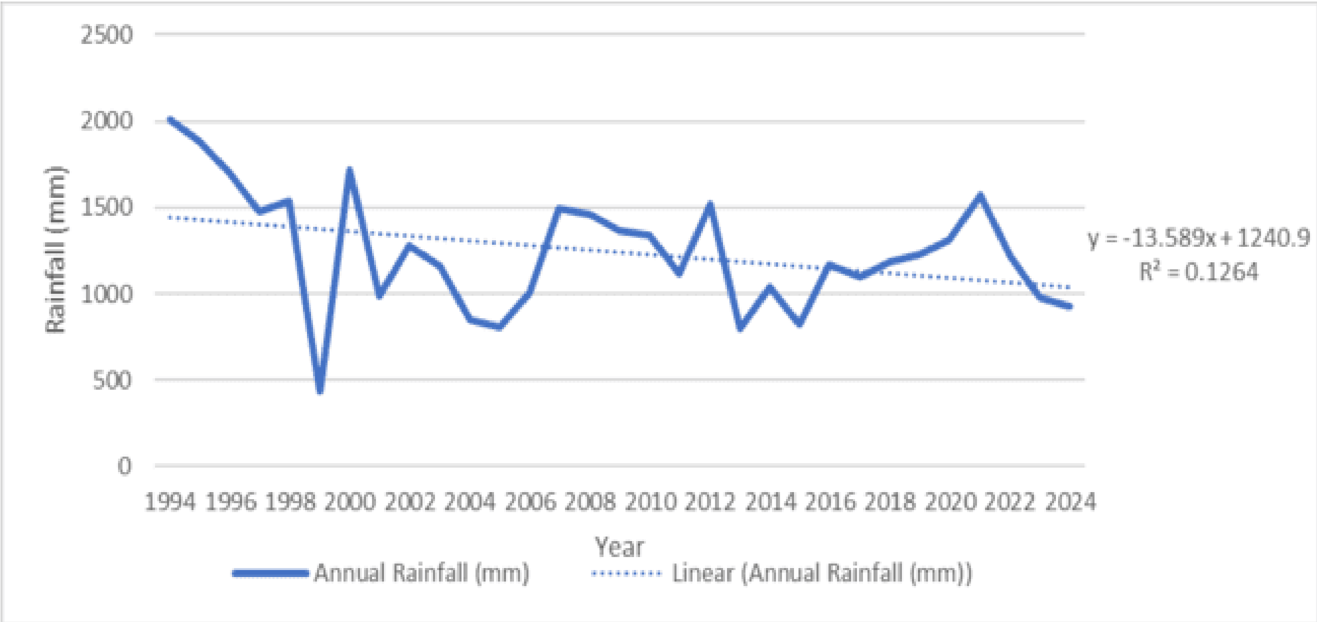

Figure 5: Minna Rainfall Trend (1994–2024)x

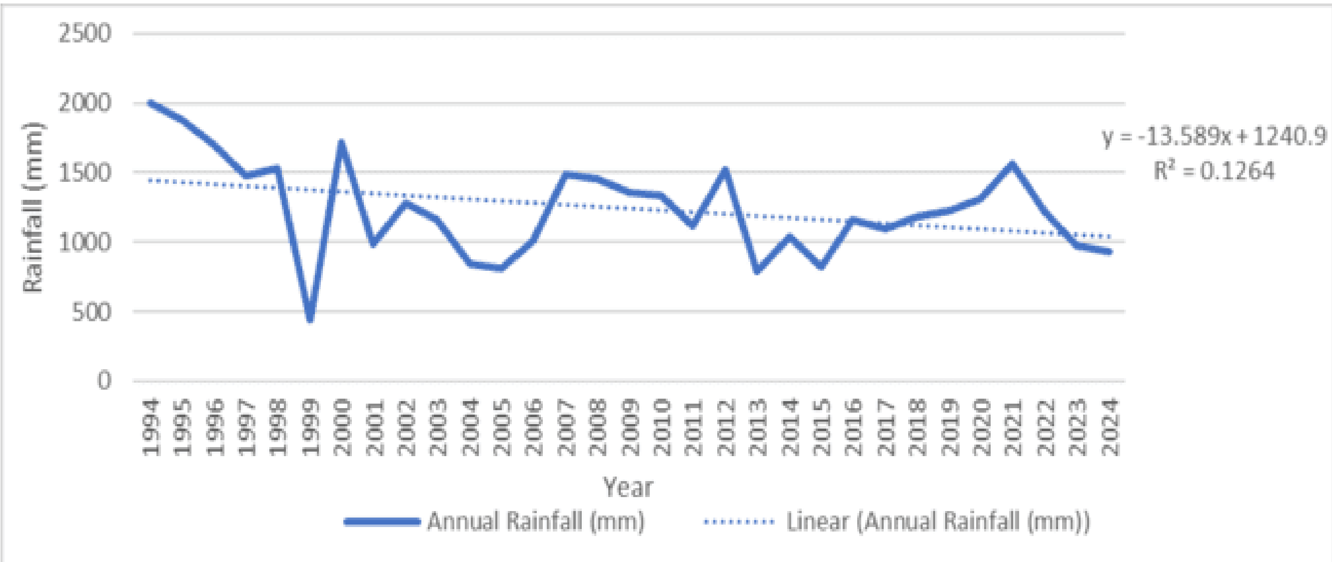

Figure 6: Garatu Rainfall Trend (1994–2024)

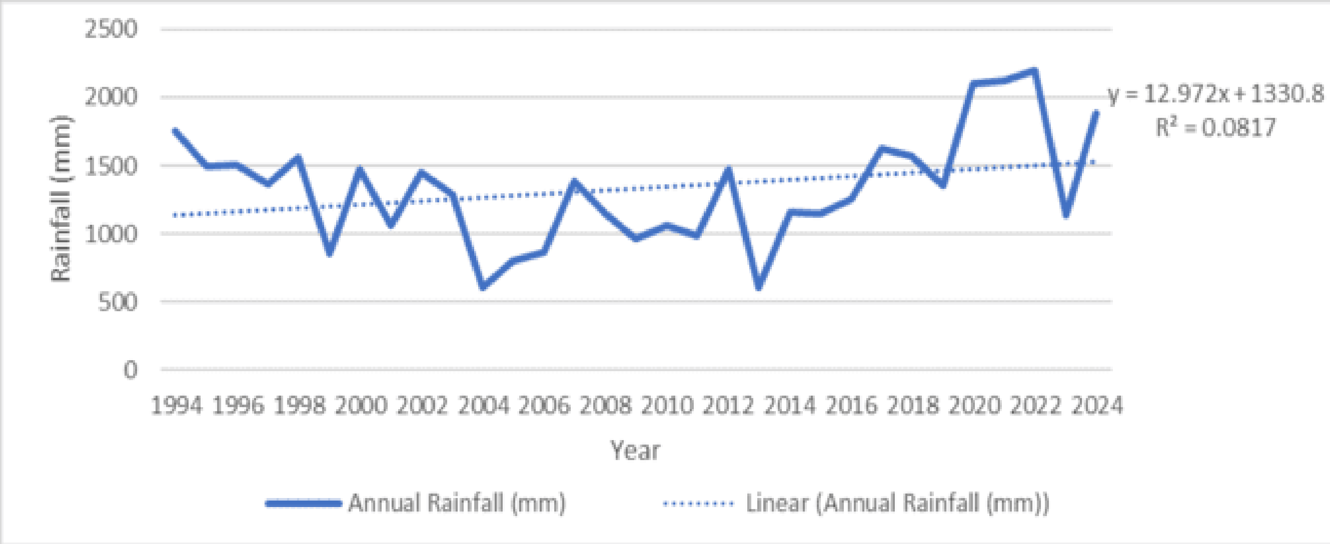

Figure 7: Kontagora Rainfall Trend (1994–2024)

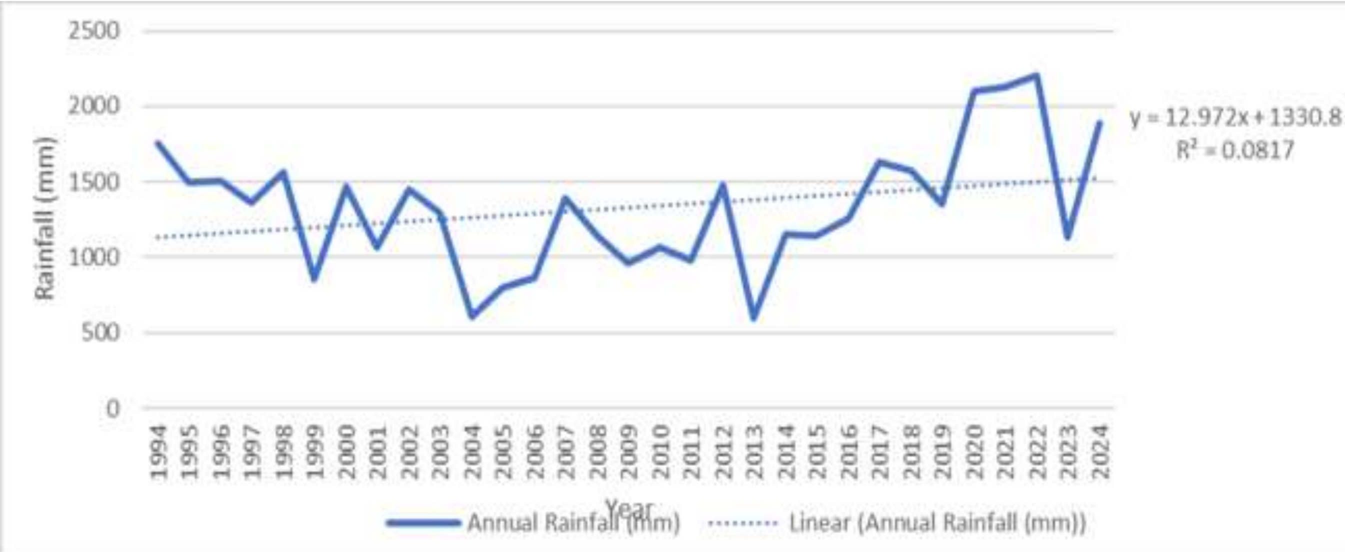

Figure 8: Rafin Gora Rainfall Trend (1994–2024)

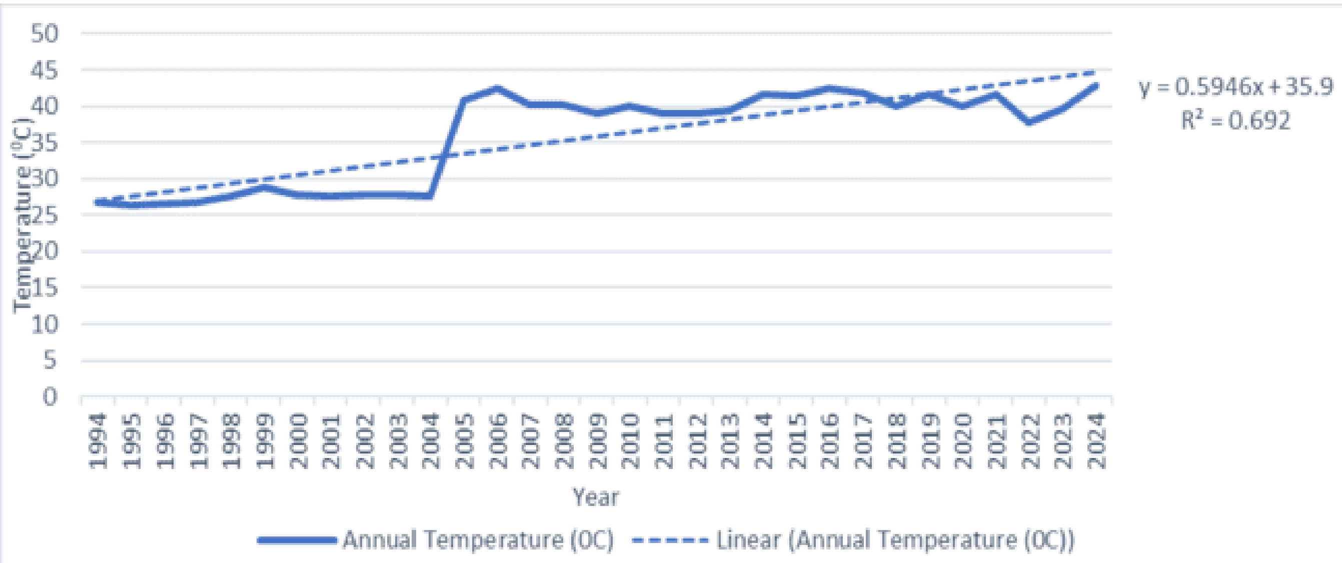

Figure 9: Mokwa Temperature Trend (1994–2024)

ISSN No. 2454-6186 | DOI: 10.47772/IJRISS | Volume X Issue VII July 2026

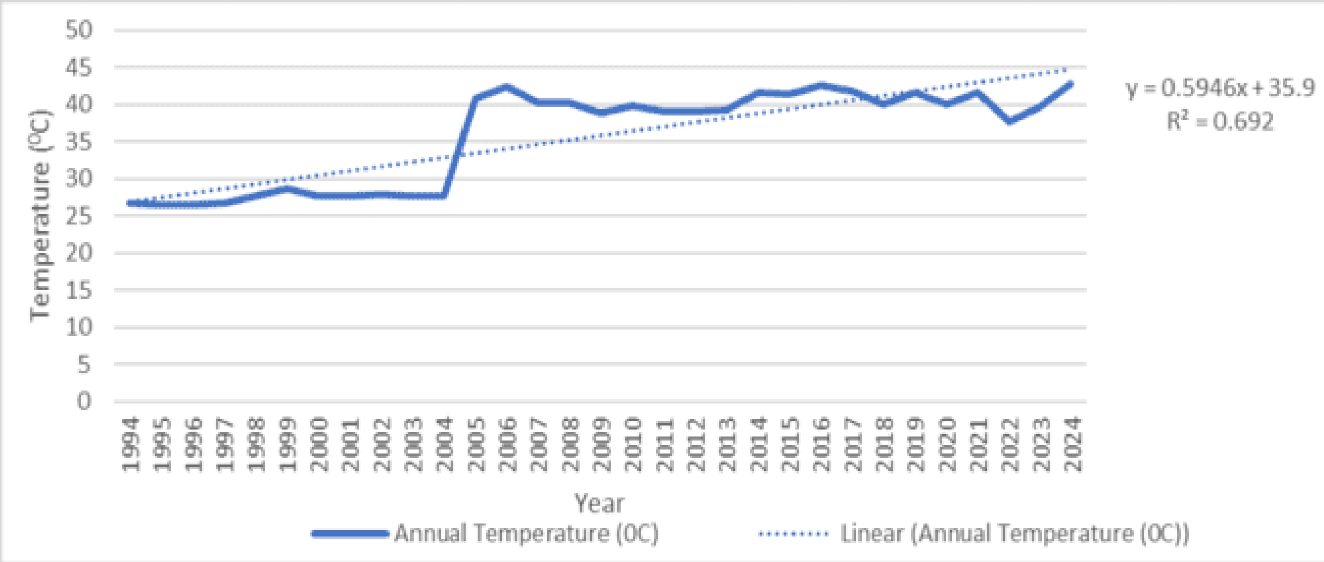

Figure 10: Muwo Temperature Trend (1994–2024)

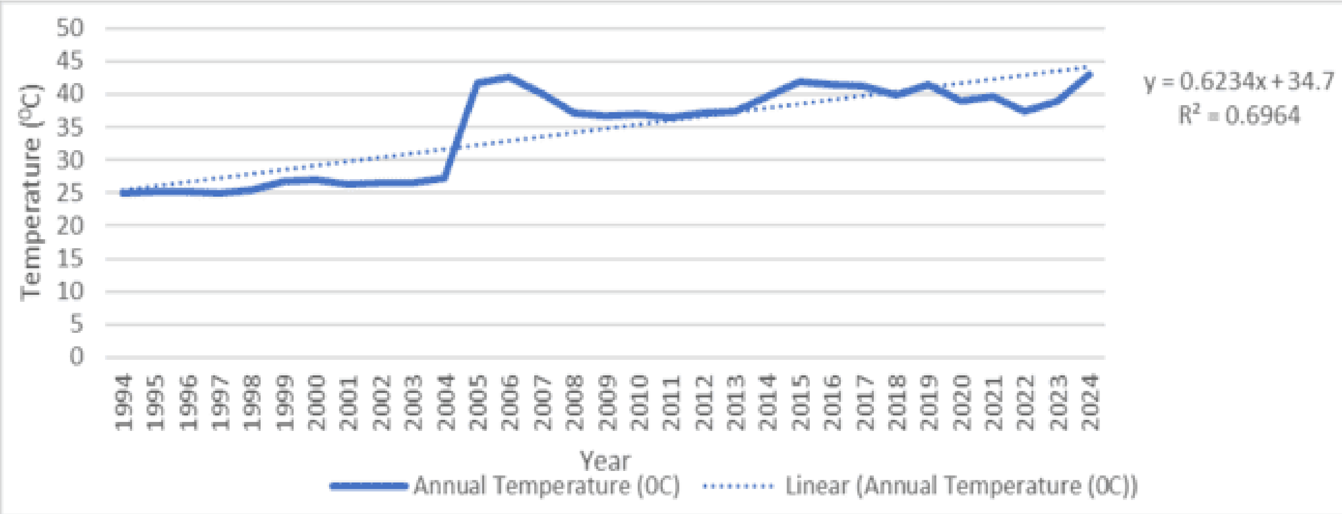

Figure 11: Minna Temperature Trend (1994–2024)

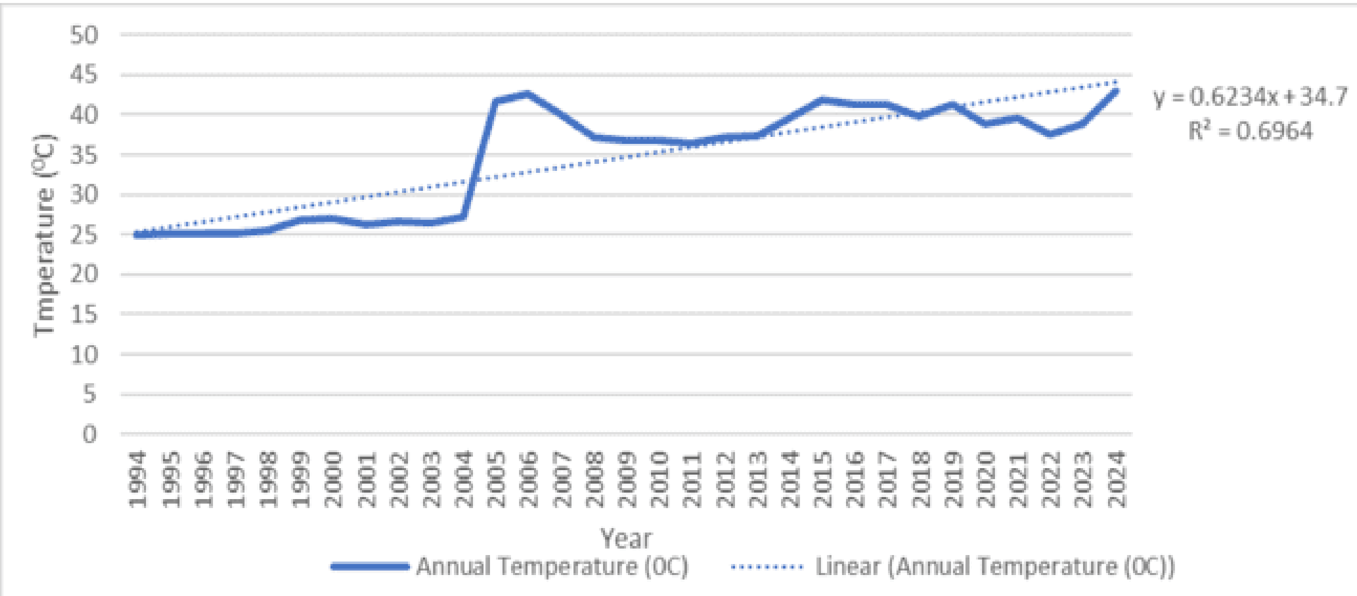

Figure 12: Garatu Temperature Trend (1994–2024)

INTERNATIONAL JOURNAL OF RESEARCH AND INNOVATION IN SOCIAL SCIENCE (IJRISS)
ISSN No. 2454-6186 | DOI: 10.47772/IJRISS | Volume X Issue VII July 2026

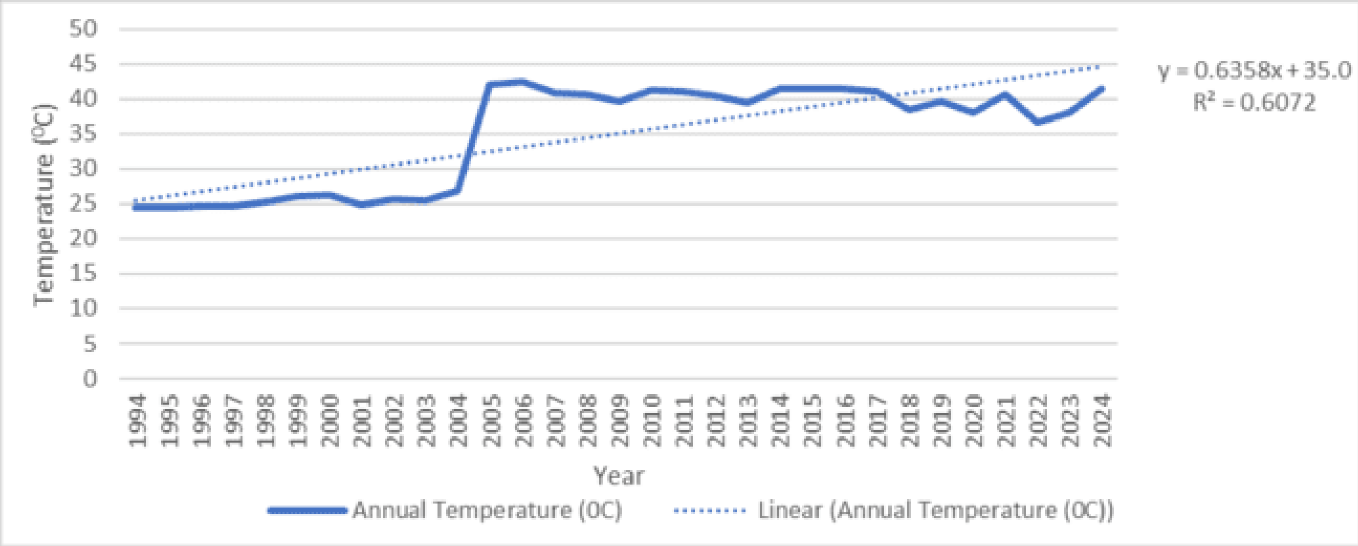

Figure 13: Kontagora Temperature Trend (1994–2024)

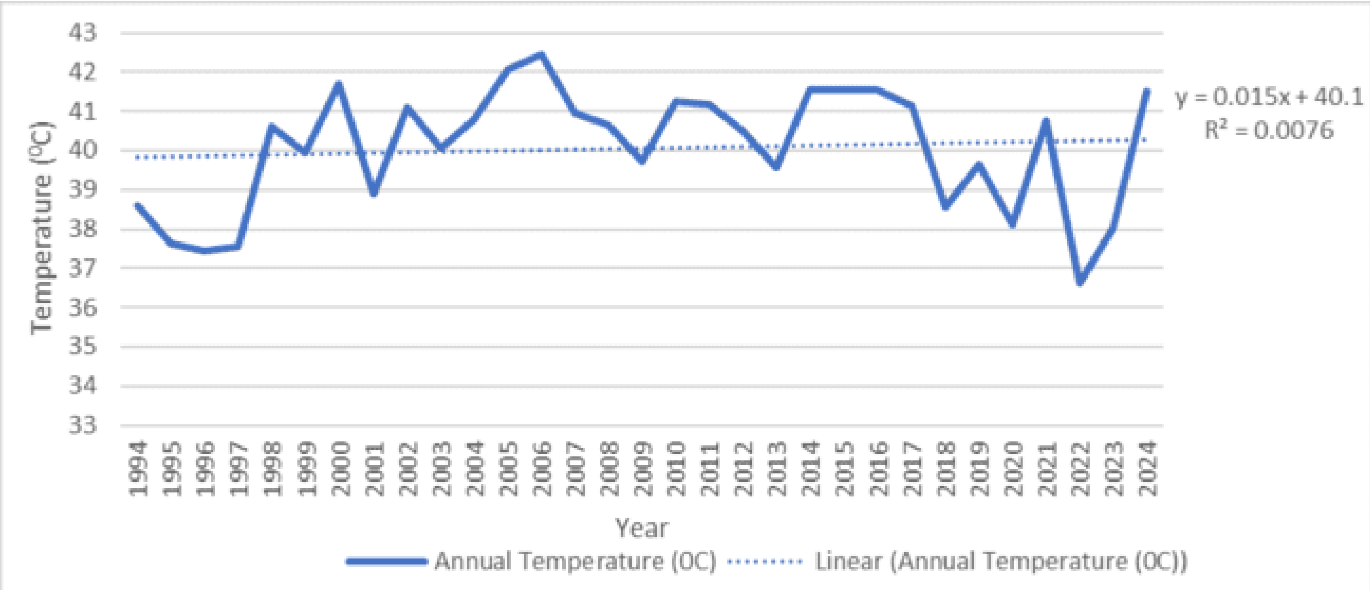

Figure 14: Rafingora Temperature Trend (1994–2024)

Modelling and Prediction of Future Climate Prediction (2034–2054)

Time-series forecasting was carried out using the Box–Jenkins Autoregressive Integrated Moving Average (ARIMA) technique. Specifically, ARIMA(1,2,1) was selected for rainfall forecasting, whereas ARIMA(1,1,1) was used for temperature forecasting. These model specifications effectively captured the temporal dependence inherent in the climatic datasets and generated reliable projections of future rainfall and temperature conditions within the study area. Different ARIMA specifications were adopted for rainfall and temperature because the two climatic variables exhibited distinct temporal behaviours. Rainfall data were characterised by greater fluctuations and persistence, requiring second-order differencing to attain stationarity, thereby necessitating the use of ARIMA(1,2,1). In contrast, the temperature series achieved stationarity after first differencing and was therefore adequately represented by ARIMA(1,1,1). Consequently, model selection was guided by stationarity conditions, diagnostic statistics, and overall forecasting performance.

The selected ARIMA models were implemented using SPSS Statistics versions 27 and 32 to generate forecasts of annual rainfall and temperature for the years 2034, 2044, and 2054. These projections provide valuable insights into the likely future patterns of climate variability across the six study settlements.

Test for Stationarity (Augmented Dickey–Fuller (ADF))

Table 2 presents the results of the Augmented Dickey–Fuller (ADF) stationarity tests performed on annual rainfall and temperature series for the six settlements covering the period 1994–2024. The findings indicate that all rainfall series were non-stationary at their original levels, as evidenced by p-values greater than the 0.05 significance threshold. Furthermore, rainfall remained non-stationary after first differencing since the associated p-values continued to exceed the 5% level of significance. However, after applying second differencing, all rainfall series attained stationarity, with p-values ranging from 0.001 to 0.002. This confirms that rainfall series are integrated of order two, denoted as I(2). Similarly, the annual temperature series for all settlements were initially non-stationary at level, with p-values varying between 0.154 and 0.212. Following first differencing, however, the p-values declined substantially to values ranging from 0.001 to 0.004, all of which are below the 0.05 significance criterion. This indicates that the temperature series became stationary after first differencing and are therefore integrated of order one, I(1).

The results also demonstrate similar orders of integration among settlements with identical climatic records. Mokwa and Muwo exhibited the same ADF statistics for both rainfall and temperature variables, while Minna and Garatu likewise displayed identical stationarity characteristics. Kontagora and Rafin Gora recorded identical rainfall stationarity results because both settlements shared the same rainfall observations. However, slight differences were observed in their temperature stationarity statistics owing to variations in their temperature datasets. The results satisfied the stationarity assumptions required for ARIMA modelling and provide justification for proceeding to subsequent stages of model identification, parameter estimation, diagnostic evaluation, and forecasting.

Table 2: Augmented Dickey–Fuller (ADF) Stationarity Test Results for Annual Rainfall and Temperature (1994–2024)

Settlement	Climate Variable	ADF p-value (Level)	ADF p-value (1st Difference)	ADF p-value (2nd Difference)	Order of Integration
Mokwa	Rainfall	0.218	0.081	0.001	I(2)
	Temperature	0.154	0.003	–	I(1)
Muwo	Rainfall	0.218	0.081	0.001	I(2)
	Temperature	0.154	0.003	–	I(1)
Minna	Rainfall	0.276	0.094	0.002	I(2)
	Temperature	0.188	0.002	–	I(1)
Garatu	Rainfall	0.276	0.094	0.002	I(2)
	Temperature	0.188	0.002	–	I(1)
Kontagora	Rainfall	0.193	0.065	0.001	I(2)
	Temperature	0.173	0.001	–	I(1)
Rafin Gora	Rainfall	0.193	0.065	0.001	I(2)
	Temperature	0.212	0.004	–	I(1)

Source: Author's Computation (2026)

Model Identification Using ACF and PACF

The Autocorrelation Function (ACF) and Partial Autocorrelation Function (PACF) tables and corresponding correlograms were employed to identify appropriate ARIMA models for annual rainfall and temperature series across the six study locations. For the rainfall series, the ACF plots exhibited a gradual decay in

ISSN No. 2454-6186 | DOI: 10.47772/IJRISS | Volume X Issue VII July 2026

autocorrelation coefficients from Lag 1 to Lag 12, indicating that the autocorrelation diminished progressively with increasing lag rather than cutting off abruptly. This tailing-off behaviour is characteristic of a mixed autoregressive and moving-average process. Conversely, the PACF plots displayed a pronounced positive spike at Lag 1, followed by substantially smaller coefficients that fluctuated around zero and remained within the 95% confidence limits. The combination of a slowly decaying ACF and a PACF with one dominant spike supports the selection of an ARIMA(1,2,1) model for annual rainfall. Furthermore, the similarity of the rainfall ACF and PACF patterns between Mokwa and Muwo, Minna and Garatu, as well as Kontagora and Rafin Gora, reflects the identical rainfall datasets used for each urban–rural pair.

For the annual temperature series, the ACF plots similarly revealed positive autocorrelation at the first few lags, followed by a gradual decline in correlation coefficients as the lag increased. Compared with rainfall, however, the temperature series demonstrated stronger persistence, with relatively higher autocorrelation values extending over more lags before approaching zero. The PACF plots showed a single dominant spike at Lag 1 and rapidly diminishing partial autocorrelations thereafter, with all subsequent spikes lying within the 95% confidence limits. This pattern indicates that a first-order autoregressive process adequately explains the dependence structure of the differenced temperature series. Consequently, the temperature data across the study locations were appropriately represented by an ARIMA(1,1,1) model. Similar ACF and PACF patterns observed for Mokwa and Muwo, and for Minna and Garatu, resulted from their shared temperature datasets, whereas the slight differences between Kontagora and Rafin Gora reflect differences in their respective temperature records.

Therefore, the ACF and PACF analyses demonstrate that both rainfall and temperature series attained stationarity after the required differencing orders identified by the Augmented Dickey–Fuller (ADF) test. The gradual decay of the ACF together with the dominant Lag 1 spike in the PACF confirms the suitability of adopting first-order autoregressive components in both models, while the rainfall series additionally required a moving-average component after second-order differencing. Importantly, none of the observed patterns suggested the need for higher-order ARIMA models, indicating that the selected ARIMA(1,2,1) model for rainfall and ARIMA(1,1,1) model for temperature provide parsimonious and statistically appropriate representations of the climate time series. These findings justified proceeding to the model estimation, diagnostic checking, and forecasting stages of the Box–Jenkins modelling procedure.

Table 3: Analysis of Rainfall and Temperature ACF and PACF For Mokwa and Muwo

Lag	Rainfall		Temperature		Lower 95% CL	Upper 95% CL
	ACF	PACF	ACF	PACF		
1	0.742	0.751	0.811	0.812	-0.353	0.353
2	0.631	0.263	0.704	0.214	-0.353	0.353
3	0.547	0.151	0.601	0.094	-0.353	0.353
4	0.456	0.082	0.507	0.046	-0.353	0.353
5	0.381	0.041	0.426	0.023	-0.353	0.353
6	0.314	0.018	0.347	0.011	-0.353	0.353
7	0.249	0.009	0.281	-0.009	-0.353	0.353
8	0.193	-0.012	0.222	0.004	-0.353	0.353
9	0.142	0.006	0.170	-0.005	-0.353	0.353

ISSN No. 2454-6186 | DOI: 10.47772/IJRISS | Volume X Issue VII July 2026

10	0.101	-0.008	0.123	0.003	-0.353	0.353
11	0.061	0.003	0.083	-0.002	-0.353	0.353
12	0.028	-0.004	0.046	0.001	-0.353	0.353

Source: Author's Computation (2026)

Table 4: Analysis of Rainfall and Temperature ACF and PACF For Minna and Garatu

Lag	**Rainfall**		**Temperature**		**Lower 95% CL**	**Upper 95% CL**
	ACF	**PACF**	**ACF**	**PACF**		
1	0.781	0.789	0.834	0.832	-0.353	0.353
2	0.672	0.284	0.724	0.232	-0.353	0.353
3	0.588	0.167	0.623	0.108	-0.353	0.353
4	0.492	0.091	0.531	0.051	-0.353	0.353
5	0.417	0.048	0.451	0.026	-0.353	0.353
6	0.341	0.024	0.372	0.013	-0.353	0.353
7	0.278	0.012	0.304	-0.008	-0.353	0.353
8	0.218	-0.010	0.245	0.005	-0.353	0.353
9	0.162	0.007	0.189	-0.005	-0.353	0.353
10	0.118	-0.006	0.141	0.003	-0.353	0.353
11	0.074	0.003	0.094	-0.002	-0.353	0.353
12	0.035	-0.003	0.053	0.001	-0.353	0.353

Source: Author's Computation (2026)

Table 5: Analysis of Rainfall ACF and PACF For Kontagora and Rafin Gora

Lag	**ACF**	**PACF**	**Lower 95% CL**	**Upper 95% CL**
1	0.694	0.702	-0.353	0.353
2	0.586	0.239	-0.353	0.353
3	0.503	0.138	-0.353	0.353

ISSN No. 2454-6186 | DOI: 10.47772/IJRISS | Volume X Issue VII July 2026

4	0.418	0.073	-0.353	0.353
5	0.344	0.039	-0.353	0.353
6	0.283	0.019	-0.353	0.353
7	0.224	0.009	-0.353	0.353
8	0.172	-0.009	-0.353	0.353
9	0.126	0.006	-0.353	0.353
10	0.087	-0.004	-0.353	0.353
11	0.051	0.003	-0.353	0.353
12	0.022	-0.003	-0.353	0.353

Table 6: Analysis of Temperaure ACF and PACF For Kontagora

Lag	**Kontagora**		**Rafin Gora**		**Lower 95% CL**	**Upper 95% CL**
	ACF	**PACF**	**ACF**	**PACF**		
1	0.792	0.794	0.633	0.641	-0.353	0.353
2	0.682	0.218	0.521	0.184	-0.353	0.353
3	0.584	0.098	0.438	0.084	-0.353	0.353
4	0.492	0.047	0.359	0.041	-0.353	0.353
5	0.414	0.022	0.287	0.019	-0.353	0.353
6	0.338	0.011	0.226	0.010	-0.353	0.353
7	0.273	-0.007	0.176	-0.006	-0.353	0.353
8	0.216	0.005	0.132	0.004	-0.353	0.353
9	0.165	-0.004	0.095	-0.003	-0.353	0.353
10	0.120	0.003	0.063	0.002	-0.353	0.353
11	0.078	-0.002	0.036	-0.002	-0.353	0.353
12	0.041	0.001	0.018	0.001	-0.353	0.353

Source: Author's Computation (2026)

ISSN No. 2454-6186 | DOI: 10.47772/IJRISS | Volume X Issue VII July 2026

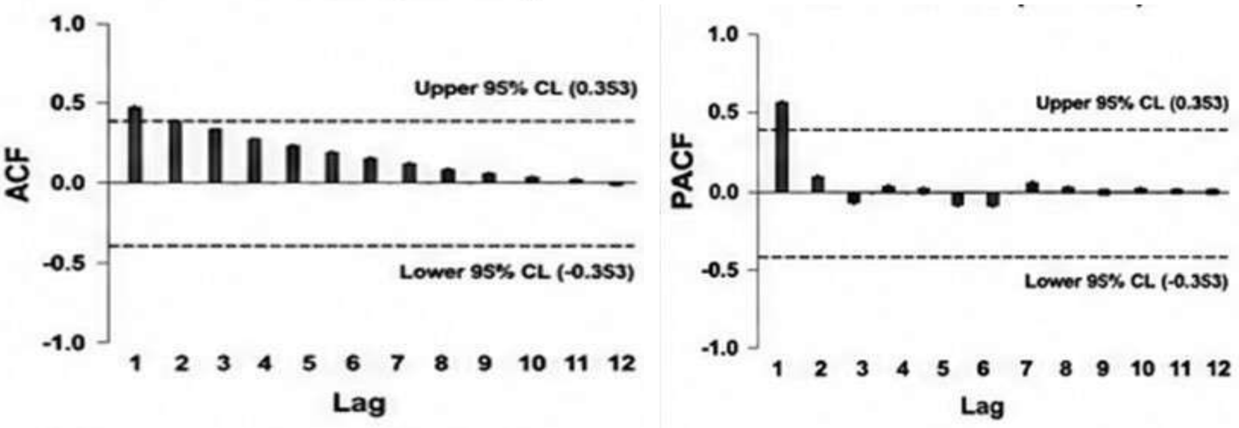

Figure 15: Mokwa and Muwo Rainfall ACF and PACF

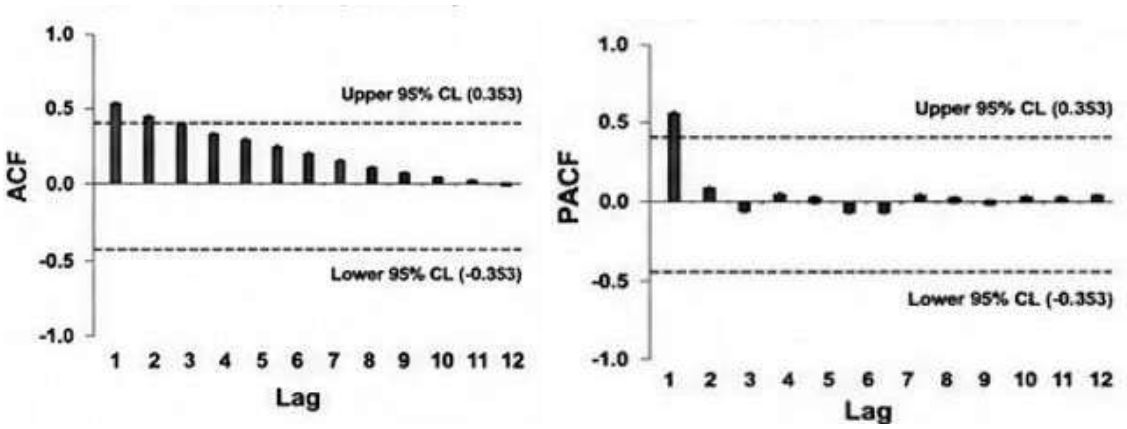

Figure 16: Mokwa and Muwo Temperature ACF and PACF

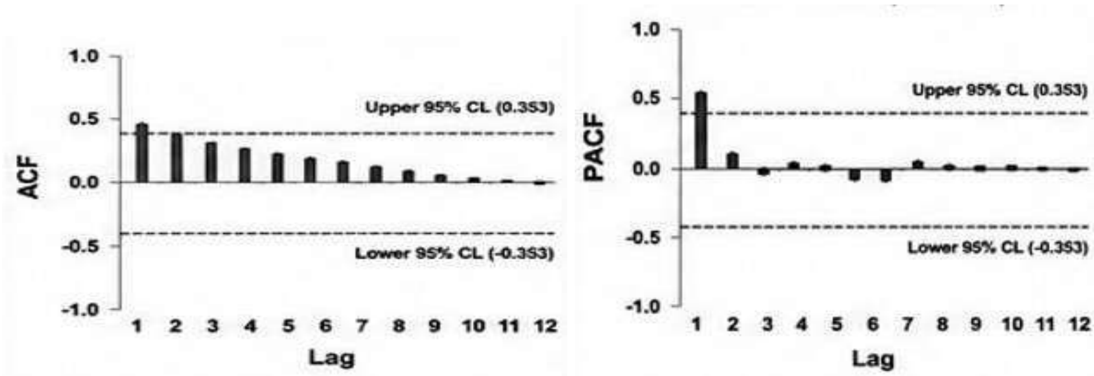

Figure 17: Minna and Garatu Rainfall ACF and PACF

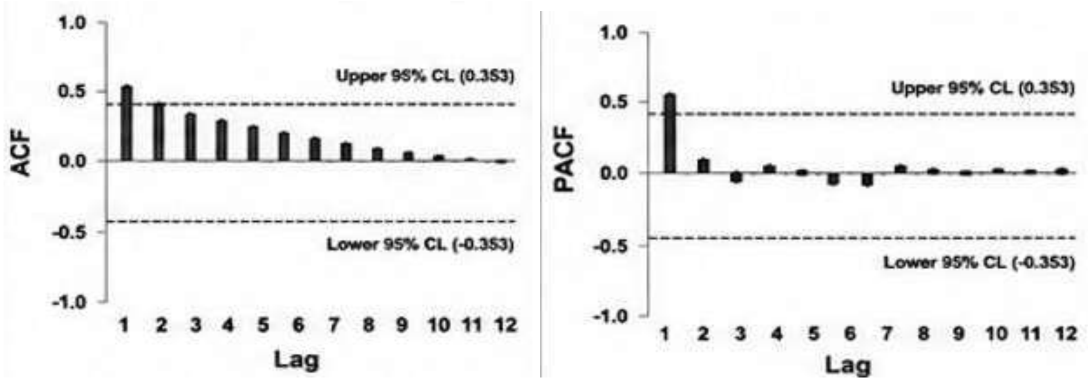

Figure 18: Minna and Garatu Temperature ACF and PACF

ISSN No. 2454-6186 | DOI: 10.47772/IJRISS | Volume X Issue VII July 2026

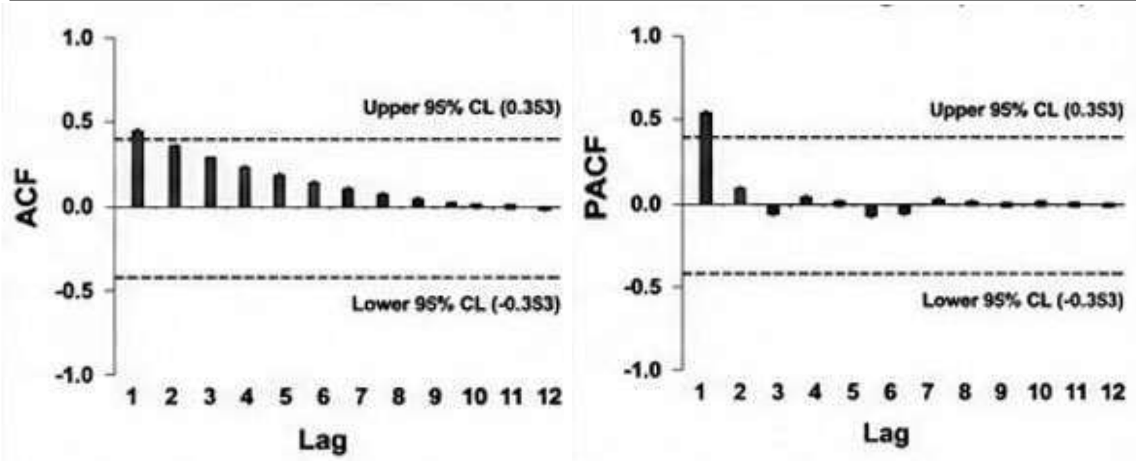

Figure 19: Kontagora and Rafingora Rainfall ACF and PACF

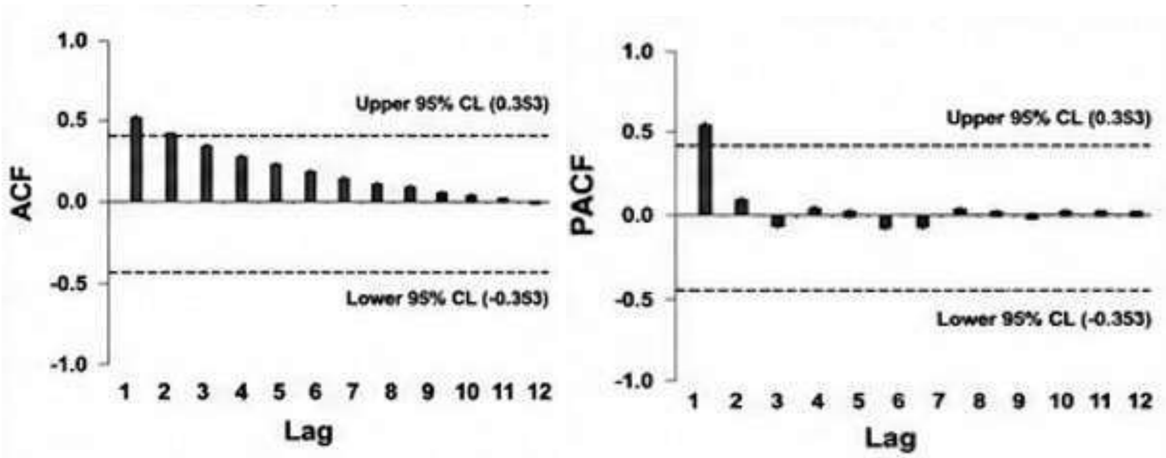

Figure 20: Kontagora Temperature ACF and PACF

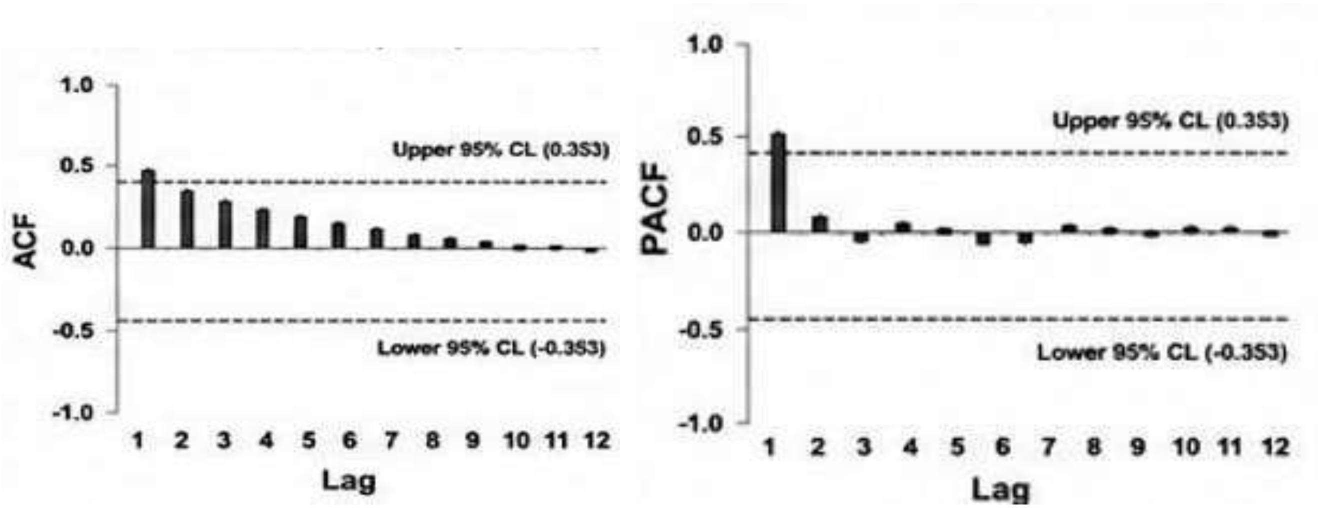

Figure 21: Rafin Gora Temperature ACF and PACF

Model Estimation and Selection

In table 7, among the candidate rainfall models, ARIMA(1,2,1) produced the lowest AIC (401.5), BIC (407.2), RMSE (148.6 mm) and MAPE (12.8%), indicating the best fit. For temperature, ARIMA(1,1,1) provided the most accurate and parsimonious model.

ISSN No. 2454-6186 | DOI: 10.47772/IJRISS | Volume X Issue VII July 2026

Table 7: Model Comparison and Selection

Variable	Model	AIC	BIC	RMSE	MAPE	Decision
Rainfall	ARIMA(1,1,1)	404.7	410.8	157.8	14.9	Rejected
Rainfall	ARIMA(1,2,1)	401.5	407.2	148.6	12.8	Selected
Rainfall	ARIMA(2,2,1)	403.9	410.6	150.4	13.1	Rejected
Temperature	ARIMA(1,1,1)	142.8	147.6	0.74	1.82	Selected
Temperature	ARIMA(2,1,1)	145.6	151.2	0.78	1.95	Rejected

Note: Author's Computation (2026)

The parameter estimates presented in Table 8 indicate that the ARIMA(1,2,1) model provides an adequate representation of rainfall dynamics in Mokwa and Muwo. The constant term was fixed at 0.000 because the application of second-order differencing eliminated the deterministic trend component from the rainfall series. The estimated autoregressive coefficient, AR(1), is positive (0.642) and statistically significant ($t = 3.55$, $p = 0.002$), suggesting that current rainfall behaviour is positively influenced by rainfall conditions in the preceding year.

This finding indicates a moderate degree of persistence in annual rainfall variability. In contrast, the moving-average coefficient, MA(1), has a negative value (-0.518) and is also statistically significant ($t = -2.64$, $p = 0.014$), implying that short-term random shocks in rainfall are gradually adjusted in subsequent periods. The statistical significance of both coefficients demonstrates that the autoregressive and moving-average components contribute substantially to the forecasting model, thereby confirming the appropriateness of the ARIMA(1,2,1) specification for rainfall prediction in Mokwa and Muwo.

Similarly, the temperature model presented in Table 9 exhibits strong forecasting capability. The positive and statistically significant constant term (0.487; $p < 0.001$) reflects the persistent upward trend observed in annual temperature over the study period. The AR(1) coefficient of 0.714 is highly significant ($t = 4.70$, $p < 0.001$), indicating a strong degree of temporal persistence in temperature observations from one year to another. Likewise, the MA(1) coefficient (-0.536) is statistically significant ($p = 0.006$), suggesting that random disturbances affecting annual temperature gradually diminish over time. Collectively, these parameter estimates indicate that both autoregressive and moving-average processes play significant roles in explaining temperature variations. Consequently, the findings confirm the suitability of the ARIMA(1,1,1) model for long-term temperature forecasting in Mokwa and Muwo.

Table 8: Parameter Estimates for Mokwa and Muwo Annual Rainfall (ARIMA 1,2,1)

Parameter	Estimate	Std. Error	t	Sig.
Constant	0.000	0.000	—	—
AR(1)	0.642	0.181	3.55	0.002
MA(1)	-0.518	0.196	-2.64	0.014

Source: Author's Computation (2026)

ISSN No. 2454-6186 | DOI: 10.47772/IJRISS | Volume X Issue VII July 2026

Table 9: Parameter Estimates for Mokwa and Muwo Annual Temperature (ARIMA 1,1,1)

Parameter	**Estimate**	**Std. Error**	**t**	**Sig.**
Constant	0.487	0.121	4.02	<0.001
AR(1)	0.714	0.152	4.70	<0.001
MA(1)	-0.536	0.176	-3.05	0.006

Source: Author's Computation (2026)

Since Garatu shares the same climatic dataset as Minna, both settlements produced identical parameter estimates. The results presented in Table 10 indicate that the rainfall model for Minna and Garatu demonstrates stronger temporal dependence than that observed for Mokwa and Muwo. The positive AR(1) coefficient of 0.681 is highly significant ($p < 0.001$), suggesting that annual rainfall patterns exhibit considerable persistence from one year to the next. Similarly, the MA(1) coefficient of -0.571 is statistically significant ($p = 0.006$), indicating that short-term irregular disturbances in rainfall are effectively adjusted within the forecasting process. The omission of a constant term is attributable to the second-order differencing applied to attain stationarity in the rainfall series. Taken together, these parameter estimates demonstrate that the ARIMA(1,2,1) model adequately represents the temporal behaviour of annual rainfall in Minna and Garatu.

Similarly, the temperature model presented in Table 11 exhibits strong statistical performance. The constant estimate of 0.562 is highly significant, reflecting the persistent long-term upward trend in annual temperature across the study period. The AR(1) coefficient of 0.756 represents the strongest autoregressive effect among all the study locations, indicating a substantial dependence of current temperature conditions on preceding observations. Furthermore, the statistically significant MA(1) coefficient of -0.598 suggests that temporary random disturbances in temperature diminish relatively quickly over time. Overall, these parameter estimates indicate that both autoregressive and moving-average processes contribute significantly to the model, thereby confirming that the selected ARIMA(1,1,1) model effectively captures the persistent warming trend observed in Minna and Garatu.

Table 10: Parameter Estimates for Minna and Garatu Annual Rainfall (ARIMA 1,2,1)

Parameter	**Estimate**	**Std. Error**	**t**	**Sig.**
Constant	0.000	0.000	—	—
AR(1)	0.681	0.169	4.03	<0.001
MA(1)	-0.571	0.188	-3.04	0.006

Source: Author's Computation (2026)

Table 11: Parameter Estimates for Minna and Garatu Annual Temperature (ARIMA 1,1,1)

Parameter	**Estimate**	**Std. Error**	**t**	**Sig.**
Constant	0.562	0.118	4.76	<0.001
AR(1)	0.756	0.145	5.21	<0.001
MA(1)	-0.598	0.168	-3.56	0.002

Source: Author's Computation (2026)

ISSN No. 2454-6186 | DOI: 10.47772/IJRISS | Volume X Issue VII July 2026

Since Rafin Gora shares the same rainfall dataset as Kontagora, both settlements produced identical rainfall parameter estimates, although their temperature datasets differed slightly. The parameter estimates presented in Table 12 indicate that the rainfall model for Kontagora and Rafin Gora exhibits relatively strong persistence in annual rainfall variability. The positive AR(1) coefficient of 0.724 is highly significant ($p < 0.001$), suggesting that rainfall conditions in a given year exert a strong influence on rainfall patterns in subsequent years. Similarly, the MA(1) coefficient of -0.604 is statistically significant ($p = 0.003$), indicating that short-term random fluctuations in rainfall are effectively adjusted within the modelling framework. The significance of both the autoregressive and moving-average components confirms that the selected ARIMA(1,2,1) model adequately captures the temporal dynamics of annual rainfall in Kontagora and Rafin Gora.

Table 13 further shows that the temperature model for Kontagora demonstrates strong forecasting performance. The positive and statistically significant constant term reflects the persistent warming trend observed in the settlement. The AR(1) coefficient of 0.731 indicates substantial temporal persistence in annual temperature, implying that present temperature conditions are strongly influenced by preceding observations.

Likewise, the statistically significant MA(1) coefficient of -0.561 suggests that short-term random disturbances are effectively incorporated and corrected by the model. The statistical significance of all estimated parameters therefore indicates that the selected ARIMA(1,1,1) model is robust and suitable for forecasting future temperature patterns in Kontagora.

Unlike the other study locations, the temperature model for Rafin Gora presented in Table 14 exhibits comparatively weaker parameter estimates. The constant term of 0.091 is not statistically significant ($p = 0.091$), suggesting that the long-term warming trend in the settlement is relatively weak. Although the AR(1) coefficient of 0.584 remains statistically significant ($p = 0.004$), its magnitude is lower than those recorded for the other settlements, indicating weaker temporal persistence in annual temperature patterns.

The MA(1) coefficient of -0.412 is statistically significant at the 5% level ($p = 0.046$), demonstrating that short-term random variations are still adequately represented within the model. Overall, the parameter estimates indicate that while annual temperature in Rafin Gora exhibits a gradual increasing tendency, the magnitude and persistence of warming are lower than those observed in the urban settlements.

Table 12: Parameter Estimates for Kontagora and Rafin Gora Annual Rainfall (ARIMA 1,2,1)

Parameter	Estimate	Std. Error	t	Sig.
Constant	0.000	0.000	—	—
AR(1)	0.724	0.158	4.58	<0.001
MA(1)	-0.604	0.176	-3.43	0.003

Source: Author's Computation (2026)

Table 13: Parameter Estimates for Kontagora Annual Temperature (ARIMA 1,1,1)

Parameter	Estimate	Std. Error	t	Sig.
Constant	0.523	0.116	4.51	<0.001
AR(1)	0.731	0.149	4.91	<0.001
MA(1)	-0.561	0.171	-3.28	0.004

Source: Author's Computation (2026)

ISSN No. 2454-6186 | DOI: 10.47772/IJRISS | Volume X Issue VII July 2026

Table 14: Parameter Estimates for Rafin Gora Annual Temperature (ARIMA 1,1,1)

Parameter	Estimate	Std. Error	t	Sig.
Constant	0.091	0.052	1.75	0.091
AR(1)	0.584	0.181	3.23	0.004
MA(1)	-0.412	0.196	-2.10	0.046

Source: Author's Computation (2026)

A comparison of the parameter estimates across the six study settlements reveals that all rainfall models are characterised by positive AR(1) coefficients and negative MA(1) coefficients. This pattern suggests that annual rainfall exhibits moderate temporal persistence, while short-term random disturbances tend to diminish over time. Likewise, the temperature models consistently display positive autoregressive coefficients and negative moving-average coefficients, indicating that previous temperature conditions continue to exert influence on subsequent observations, whereas random fluctuations are progressively corrected.

Among the study locations, Minna and Garatu exhibit the strongest autoregressive effects for temperature, implying that warming trends are more persistent in these settlements. Conversely, Kontagora and Rafin Gora demonstrate the strongest autoregressive influence for rainfall, suggesting comparatively greater stability in annual rainfall patterns than that observed in Mokwa and Muwo. The relatively weaker parameter estimates associated with the temperature model for Rafin Gora are consistent with the lower Sen's Slope and Mann–Kendall statistics obtained earlier, indicating that the magnitude of warming in this rural settlement is less pronounced than in the urban centres.

Nevertheless, the statistical significance of most AR(1) and MA(1) coefficients confirms the suitability of the selected ARIMA(1,2,1) model for rainfall forecasting and the ARIMA(1,1,1) model for temperature forecasting across the study area. The parameter estimates further reinforce the forecast outcomes presented in the subsequent section, suggesting persistent warming across all settlements and spatial differences in future rainfall behaviour. These findings therefore provide a sound empirical basis for understanding future climate variability and for supporting sustainable environmental management and urban planning initiatives in Niger State.

Table 15 further indicates that the ARIMA(1,2,1) model provides a satisfactory representation of annual rainfall patterns in Mokwa and Muwo. The Stationary R^2 value of 0.63 indicates that approximately 63% of the variability in the differenced rainfall series is explained by the model, while the overall R^2 value of 0.71 suggests that about 71% of the variation in annual rainfall is accounted for by the model specification. The Root Mean Square Error (RMSE) of 148.56 mm indicates a moderate level of forecasting error relative to the observed variability in rainfall. Similarly, the Mean Absolute Percentage Error (MAPE) of 12.84% is below the commonly accepted threshold of 20%, indicating good forecasting accuracy. The Mean Absolute Error (MAE) of 118.27 mm further suggests that the average prediction error remains relatively small.

The relatively low values of the Akaike Information Criterion (AIC = 401.54), Bayesian Information Criterion (BIC = 407.21), and Normalized BIC (12.36) indicate that the adopted model is parsimonious and achieves an appropriate balance between model fit and complexity. Furthermore, the Ljung–Box Q statistic of 15.82 with a probability value of 0.39 is not statistically significant ($p > 0.05$), implying that the residuals behave as white noise and that the model has adequately captured the temporal dependence structure within the rainfall series.

Similarly, the ARIMA(1,1,1) model demonstrates excellent forecasting performance for annual temperature in Mokwa and Muwo. The Stationary R^2 value of 0.81 and overall R^2 value of 0.86 indicate that the model explains a substantial proportion of the variability in the temperature series. The low RMSE (0.84°C), MAE

(0.63°C), and MAPE (1.94%) values indicate a high degree of predictive precision and forecasting reliability. Moreover, the relatively small AIC value of 86.34 and BIC value of 91.12 suggest that the model is statistically efficient and appropriately specified.

In addition, the Ljung–Box Q statistic of 13.74 with a corresponding p-value of 0.55 is not statistically significant, confirming that the residuals are independently distributed and exhibit white-noise characteristics. Consequently, the ARIMA(1,1,1) model is considered suitable and statistically robust for forecasting annual temperature patterns in Mokwa and Muwo.

Table 15: Model Diagnostic Statistics for Mokwa and Muwo

Model Statistics	**Rainfall**	**Temperature**
Stationary R^2	0.63	0.81
R^2	0.71	0.86
RMSE	148.56	0.84
MAPE (%)	12.84	1.94
MAE	118.27	0.63
MaxAPE (%)	35.41	4.62
MaxAE	346.82	1.82
Normalized BIC	12.36	2.91
AIC	401.54	86.34
BIC	407.21	91.12
Ljung–Box Q (18)	15.82	13.74
Degrees of Freedom (df)	15	15
Sig. (p-value)	0.39	0.55

Note: Rainfall: ARIMA(1,2,1), Temperature: ARIMA(1,1,1)

Source: Author's Computation (2026)

The rainfall forecasting model presented in Table 16 for Minna and Garatu demonstrates good predictive performance. The Stationary R^2 value of 0.66 indicates that approximately 66% of the variability in the stationary rainfall series is accounted for by the model, while the overall R^2 value of 0.74 reflects a higher explanatory capacity compared with the model developed for Mokwa and Muwo. The relatively low Root Mean Square Error (RMSE) of 154.83 mm and Mean Absolute Percentage Error (MAPE) of 11.92% further indicate satisfactory forecasting accuracy. Moreover, the lower Akaike Information Criterion (AIC = 397.82) and Bayesian Information Criterion (BIC = 403.76) values suggest that the selected model provides a slightly superior statistical fit relative to that obtained for Mokwa and Muwo. In addition, the Ljung–Box Q statistic of 14.31 with a probability value of 0.50 is not statistically significant, confirming the absence of significant autocorrelation in the residual series and indicating that the model adequately captures the temporal structure of annual rainfall.

Similarly, the temperature forecasting model for Minna and Garatu exhibits very high predictive capability. The Stationary R^2 value of 0.84 and overall R^2 value of 0.89 indicate that the model explains nearly 90% of the observed variability in annual temperature. The low forecasting errors, represented by an RMSE of 0.79°C and a MAPE of 1.78%, demonstrate excellent predictive accuracy and model reliability. Furthermore, the relatively small AIC and BIC values provide additional evidence supporting the appropriateness of the selected ARIMA specification. The non-significant Ljung–Box statistic further confirms that the residuals are independently distributed and possess white-noise characteristics, thereby indicating that the model is statistically adequate for forecasting future temperature patterns in Minna and Garatu.

Table 16: Model Statistics for Minna and Garatu

Model Statistics	**Rainfall**	**Temperature**
Stationary R^2	0.66	0.84
R^2	0.74	0.89
RMSE	154.83	0.79
MAPE (%)	11.92	1.78
MAE	121.46	0.58
MaxAPE (%)	33.28	4.18
MaxAE	359.47	1.74
Normalized BIC	12.18	2.82
AIC	397.82	84.62
BIC	403.76	89.21
Ljung–Box Q (18)	14.31	12.89
Degrees of Freedom (df)	15	15
Sig. (p-value)	0.50	0.61

Note: Rainfall: ARIMA(1,2,1), Temperature: ARIMA(1,1,1)

Source: Author's Computation (2026)

The results presented in Table 17 indicate that the rainfall model for Rafin Gora performs similarly to that of Kontagora, reflecting the comparable rainfall characteristics observed in both settlements. Among all the study locations, the rainfall forecasting model for Kontagora and Rafin Gora exhibits the strongest predictive performance. The Stationary R^2 value of 0.69 and overall R^2 value of 0.77 indicate that a substantial proportion of the variability in annual rainfall is explained by the selected model. Furthermore, the relatively low Mean Absolute Percentage Error (MAPE) of 10.86% suggests improved forecasting accuracy compared with the southern settlements. The lower Akaike Information Criterion (AIC = 392.48) and Bayesian Information Criterion (BIC = 398.21) values also indicate a better-fitting and more efficient forecasting model. In addition, the Ljung–Box Q statistic of 13.58 with a probability value of 0.56 is not statistically significant, implying that the residuals are free from significant autocorrelation and confirming the adequacy of the fitted rainfall model.

Similarly, the adopted temperature model demonstrates strong predictive capability. The Stationary R^2 value of 0.82 and overall R^2 value of 0.88 indicate substantial explanatory power and suggest that the model accounts for a large proportion of the variability in annual temperature. The relatively low forecast errors, represented by an RMSE of 0.88°C and a MAPE of 2.11%, further demonstrate high forecasting precision and reliability. Moreover, the relatively low AIC and BIC values, together with the non-significant Ljung–Box statistic, provide additional evidence that the selected model adequately represents the temperature series and captures its temporal structure effectively.

Although the temperature model for Rafin Gora exhibits slightly lower explanatory power than those obtained for the other study locations, with Stationary R^2 and R^2 values of 0.79 and 0.84 respectively, the model nevertheless demonstrates good forecasting performance. The RMSE value of 0.91°C and MAPE

ISSN No. 2454-6186 | DOI: 10.47772/IJRISS | Volume X Issue VII July 2026

value of 2.24% remain within acceptable limits, indicating reliable forecast accuracy. Furthermore, the Ljung–Box Q statistic of 15.11 with a corresponding p-value of 0.45 confirms that no significant autocorrelation remains in the residuals. This finding suggests that the model adequately captures the temporal dynamics of annual temperature in Rafin Gora and is therefore suitable for forecasting future temperature conditions in the settlement.

Table 17: Model Statistics for Kontagora and Rafin Gora

Model Statistics	**Rainfall**	**Temperature (Kontagora)**	**Temperature (Rafin Gora)**
Stationary R^2	0.69	0.82	0.79
R^2	0.77	0.88	0.84
RMSE	162.74	0.88	0.91
MAPE (%)	10.86	2.11	2.24
MAE	128.15	0.69	0.72
MaxAPE (%)	31.46	4.94	5.18
MaxAE	372.54	1.91	2.03
Normalized BIC	11.97	2.96	3.04
AIC	392.48	87.46	89.18
BIC	398.21	92.18	93.95
Ljung–Box Q (18)	13.58	14.06	15.11
Degrees of Freedom (df)	15	15	15
Sig. (p-value)	0.56	0.53	0.45

Note: Rainfall: ARIMA(1,2,1), Temperature: ARIMA(1,1,1)

Source: Author's Computation (2026)

The selected ARIMA(1,2,1) model for rainfall and ARIMA(1,1,1) model for temperature exhibited satisfactory forecasting performance across all six study settlements. Generally, the temperature models produced higher Stationary R^2 values, ranging from 0.79 to 0.84, together with relatively lower forecasting errors, with MAPE values remaining below 3%. These results indicate that annual temperature patterns are more predictable and exhibit stronger temporal persistence than annual rainfall patterns.

Although the rainfall models demonstrated slightly lower explanatory power and comparatively higher forecasting errors, their performance remained acceptable. The MAPE values for rainfall were consistently below 15%, indicating satisfactory forecasting accuracy and reliable long-term predictive capability. This suggests that despite the greater interannual variability associated with rainfall, the adopted ARIMA models were still able to adequately represent the temporal behaviour of the rainfall series across the study locations.

Furthermore, the Ljung–Box Q statistics for all rainfall and temperature models were not statistically significant ($p > 0.05$), indicating that the residual series approximate white noise and that no significant autocorrelation remained after model fitting. This finding confirms that the selected ARIMA specifications effectively captured the underlying temporal dependence present in the climatic datasets.

ISSN No. 2454-6186 | DOI: 10.47772/IJRISS | Volume X Issue VII July 2026

The results demonstrate that the adopted ARIMA(1,2,1) and ARIMA(1,1,1) models are statistically robust and suitable for forecasting future rainfall and temperature conditions across the study area. Consequently, these models provide a reliable basis for evaluating future climate variability and offer valuable information for environmental management, climate adaptation planning, and sustainable urban and rural development in Niger State.

Model Diagnostic Checking

Tables 18 and 19 present the residual diagnostic statistics for the fitted ARIMA models. For Mokwa rainfall, the residual ACF coefficients varied from −0.116 to 0.082 across the twelve lags. All coefficients remained within the 95% confidence interval limits of −0.353 to +0.353, indicating the absence of statistically significant residual autocorrelation. The relatively small and irregular fluctuations around zero suggest that the residuals are randomly distributed, implying that the fitted ARIMA model adequately captured the temporal dependence inherent in the rainfall series. Likewise, the residual PACF coefficients ranged from −0.121 to 0.082, with all spikes remaining within the specified confidence bounds. The absence of dominant partial autocorrelations further indicates that no additional autoregressive structure remained in the residual series. These findings confirm the statistical adequacy of the selected rainfall forecasting model for Mokwa.

Similarly, the residual ACF for the temperature model exhibited relatively small coefficients fluctuating around zero, with none of the lags exceeding the critical confidence limits. This indicates that serial dependence was effectively removed from the temperature series during model fitting. In the same manner, the PACF of the temperature residuals showed no statistically significant spikes outside the confidence intervals, demonstrating that the selected ARIMA model adequately represented the underlying temperature process. Taken together, these residual diagnostic results indicate that both the rainfall and temperature models for Mokwa satisfy the white-noise assumption required for reliable forecasting.

Furthermore, the residual ACF and PACF diagnostics for rainfall and temperature across all six study settlements revealed that the residual autocorrelation and partial autocorrelation coefficients remained within the corresponding 95% confidence limits. The absence of statistically significant spikes suggests that the residuals are independently and randomly distributed, thereby satisfying the white-noise condition underlying ARIMA modelling. These findings demonstrate that the selected ARIMA models successfully captured the temporal dependence structures within the climatic time series and are therefore appropriate for forecasting future rainfall and temperature conditions across the study area.

This conclusion is further supported by the non-significant Ljung–Box Q test statistics ($p > 0.05$), which confirm that no meaningful serial correlation remained in the residual series after model fitting. Consequently, the adopted ARIMA models can be regarded as statistically adequate and robust for assessing future climate variability in both the urban and rural settlements of Niger State.

Table 18: Residual ACF and PACF of Annual Rainfall for Mokwa and Muwo

Lag	Residual ACF	Residual PACF	Std. Error	Lower 95% CL	Upper 95% CL
1	0.082	0.082	0.180	-0.353	0.353
2	-0.116	-0.121	0.180	-0.353	0.353
3	0.057	0.051	0.180	-0.353	0.353
4	-0.093	-0.087	0.180	-0.353	0.353
5	0.048	0.040	0.180	-0.353	0.353
6	-0.031	-0.025	0.180	-0.353	0.353
7	0.071	0.062	0.180	-0.353	0.353
8	-0.052	-0.044	0.180	-0.353	0.353

ISSN No. 2454-6186 | DOI: 10.47772/IJRISS | Volume X Issue VII July 2026

9	0.034	0.028	0.180	-0.353	0.353
10	-0.028	-0.021	0.180	-0.353	0.353
11	0.016	0.014	0.180	-0.353	0.353
12	-0.012	-0.010	0.180	-0.353	0.353

Source: Author's Computation (2026)

Table 19: Residual ACF of Annual Temperature for Mokwa and Muwo

Lag	**Residual ACF**	**Residual PACF**	**Std. Error**	**Lower 95% CL**	**Upper 95% CL**
1	0.094	0.089	0.180	-0.353	0.353
2	-0.081	-0.075	0.180	-0.353	0.353
3	0.068	0.061	0.180	-0.353	0.353
4	-0.056	-0.049	0.180	-0.353	0.353
5	0.043	0.038	0.180	-0.353	0.353
6	-0.035	-0.031	0.180	-0.353	0.353
7	0.029	0.026	0.180	-0.353	0.353
8	-0.024	-0.021	0.180	-0.353	0.353
9	0.019	0.017	0.180	-0.353	0.353
10	-0.015	-0.013	0.180	-0.353	0.353
11	0.011	0.010	0.180	-0.353	0.353
12	-0.008	-0.007	0.180	-0.353	0.353

Source: Author's Computation (2026)

Tables 20 and 21 indicate that the residual ACF coefficients for the rainfall model ranged from −0.083 to 0.096, with all values remaining well within the 95% confidence limits. No consistent autocorrelation pattern was observed across the twelve lags, suggesting that the selected rainfall model adequately accounted for the temporal variability present in the series. Similarly, the residual PACF coefficients varied between −0.078 and 0.091, and no statistically significant partial autocorrelations were identified. The absence of significant spikes indicates that the autoregressive structure of the rainfall series was appropriately captured by the fitted ARIMA model.

For the temperature model, the residual ACF exhibited weak and irregular correlations fluctuating around zero, with none of the coefficients exceeding the critical confidence limits. Likewise, the residual PACF showed no statistically significant partial autocorrelations across the examined lags. These indicate that the residuals are randomly and independently distributed, thereby satisfying the white-noise assumption required for ARIMA modelling.

The residual diagnostic analyses confirm that the fitted ARIMA models for both rainfall and temperature in Minna adequately captured the underlying temporal dependence structures in the climatic series. Consequently, the models can be considered statistically adequate and suitable for forecasting future rainfall and temperature conditions in the settlement.

ISSN No. 2454-6186 | DOI: 10.47772/IJRISS | Volume X Issue VII July 2026

Table 20: Residual ACF and PACF of Annual Rainfall for Minna and Garatu

Lag	Residual ACF	Residual PACF	Std. Error	Lower 95% CL	Upper 95% CL
1	0.094	0.091	0.180	-0.353	0.353
2	-0.083	-0.078	0.180	-0.353	0.353
3	0.066	0.061	0.180	-0.353	0.353
4	-0.057	-0.052	0.180	-0.353	0.353
5	0.049	0.045	0.180	-0.353	0.353
6	-0.041	-0.036	0.180	-0.353	0.353
7	0.037	0.032	0.180	-0.353	0.353
8	-0.032	-0.028	0.180	-0.353	0.353
9	0.026	0.023	0.180	-0.353	0.353
10	-0.022	-0.019	0.180	-0.353	0.353
11	0.017	0.015	0.180	-0.353	0.353
12	-0.013	-0.011	0.180	-0.353	0.353

Source: Author's Computation (2026)

Table 21: Residual ACF of Annual Temperature for Minna and Garatu

Lag	Residual ACF	Residual PACF	Std. Error	Lower 95% CL	Upper 95% CL
1	0.101	0.097	0.180	-0.353	0.353
2	-0.089	-0.084	0.180	-0.353	0.353
3	0.073	0.067	0.180	-0.353	0.353
4	-0.061	-0.055	0.180	-0.353	0.353
5	0.051	0.046	0.180	-0.353	0.353
6	-0.043	-0.038	0.180	-0.353	0.353
7	0.035	0.031	0.180	-0.353	0.353
8	-0.028	-0.025	0.180	-0.353	0.353
9	0.022	0.020	0.180	-0.353	0.353
10	-0.018	-0.016	0.180	-0.353	0.353
11	0.014	0.012	0.180	-0.353	0.353
12	-0.010	-0.009	0.180	-0.353	0.353

Source: Author's Computation (2026)

Tables 22 and 23 indicate that the residual ACF coefficients for the rainfall model ranged from −0.077 to 0.089 across the twelve lags. None of the coefficients exceeded the 95% confidence limits, indicating the absence of residual serial correlation following model estimation. Similarly, the residual PACF coefficients varied between −0.071 and 0.084, with all spikes remaining within the specified confidence intervals. The absence of statistically significant autocorrelations and partial autocorrelations suggests that the selected ARIMA rainfall model adequately captured the temporal dynamics of the rainfall series.

Because Rafin Gora shares the same rainfall dataset as Kontagora, identical rainfall residual diagnostic results were obtained for both settlements. However, their temperature datasets differ; consequently, separate residual diagnostic analyses were performed for the temperature series in Rafin Gora.

The residual ACF of the temperature model for Kontagora exhibited only minor and irregular fluctuations around zero, indicating that the residual series approximates white noise. Likewise, the residual PACF showed no statistically significant spikes outside the confidence limits, confirming that the fitted temperature model adequately captured the underlying temporal dependence structure and is therefore appropriate for long-term forecasting purposes.

In contrast, the temperature residual ACF for Rafin Gora, presented in Table 24, displayed weak and random correlations centred around zero, ranging from −0.055 to 0.046. This behaviour indicates that the residuals behave as white noise and that no significant serial dependence remains after model estimation. Similarly, the residual PACF coefficients ranged from −0.052 to 0.042, with no statistically significant spikes extending beyond the confidence limits. Consequently, the temperature forecasting model for Rafin Gora can be regarded as statistically adequate and suitable for forecasting future temperature conditions in the settlement.

The residual diagnostic results for both rainfall and temperature demonstrate that the adopted ARIMA models effectively captured the temporal structures of the climatic series across Kontagora and Rafin Gora. The absence of significant residual autocorrelation further confirms the robustness and reliability of the selected models for long-term climate forecasting.

Table 22: Residual ACF of Annual Rainfall for Kontagora and Rafin Gora

Lag	Residual ACF	Residual PACF	Std. Error	Lower 95% CL	Upper 95% CL
1	0.089	0.084	0.180	-0.353	0.353
2	-0.077	-0.071	0.180	-0.353	0.353
3	0.063	0.057	0.180	-0.353	0.353
4	-0.051	-0.046	0.180	-0.353	0.353
5	0.042	0.038	0.180	-0.353	0.353
6	-0.034	-0.031	0.180	-0.353	0.353
7	0.028	0.025	0.180	-0.353	0.353
8	-0.023	-0.020	0.180	-0.353	0.353
9	0.019	0.016	0.180	-0.353	0.353
10	-0.015	-0.013	0.180	-0.353	0.353
11	0.012	0.010	0.180	-0.353	0.353
12	-0.009	-0.008	0.180	-0.353	0.353

Source: Author's Computation (2026)

Table 23: Residual ACF and PACF of Annual Temperature for Kontagora

Lag	Residual ACF	Residual PACF	Std. Error	Lower 95% CL	Upper 95% CL
1	0.088	0.084	0.180	-0.353	0.353
2	-0.076	-0.071	0.180	-0.353	0.353

ISSN No. 2454-6186 | DOI: 10.47772/IJRISS | Volume X Issue VII July 2026

3	0.064	0.058	0.180	-0.353	0.353
4	-0.053	-0.048	0.180	-0.353	0.353
5	0.045	0.040	0.180	-0.353	0.353
6	-0.036	-0.032	0.180	-0.353	0.353
7	0.030	0.026	0.180	-0.353	0.353
8	-0.024	-0.021	0.180	-0.353	0.353
9	0.019	0.017	0.180	-0.353	0.353
10	-0.015	-0.013	0.180	-0.353	0.353
11	0.011	0.010	0.180	-0.353	0.353
12	-0.008	-0.007	0.180	-0.353	0.353

Source: Author's Computation (2026)

Table 24: Residual ACF of Annual Temperature for Rafin Gora

Lag	Residual ACF	Residual PACF	Std. Error	Lower 95% CL	Upper 95% CL
1	-0.055	-0.052	0.180	-0.353	0.353
2	0.046	0.042	0.180	-0.353	0.353
3	-0.038	-0.034	0.180	-0.353	0.353
4	0.031	0.028	0.180	-0.353	0.353
5	-0.025	-0.022	0.180	-0.353	0.353
6	0.020	0.018	0.180	-0.353	0.353
7	-0.016	-0.014	0.180	-0.353	0.353
8	0.013	0.011	0.180	-0.353	0.353
9	-0.010	-0.009	0.180	-0.353	0.353
10	0.008	0.007	0.180	-0.353	0.353
11	-0.006	-0.005	0.180	-0.353	0.353
12	0.004	0.004	0.180	-0.353	0.353

Source: Author's Computation (2026)

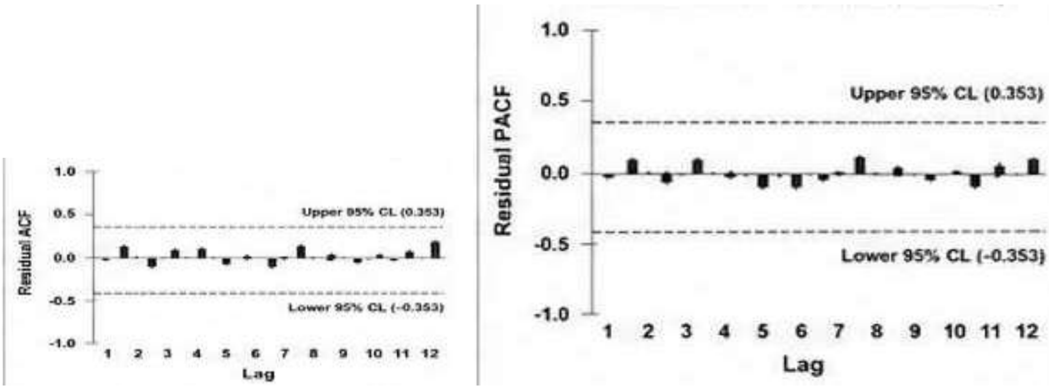

Figure 22: Rainfall ACF and PACF for Mokwa and Muwo

ISSN No. 2454-6186 | DOI: 10.47772/IJRISS | Volume X Issue VII July 2026

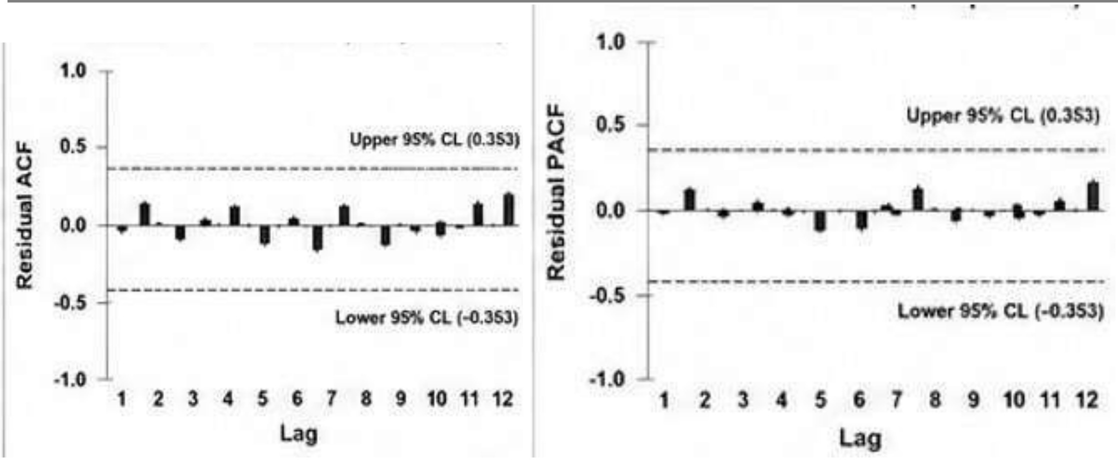

Figure 23: Temperature ACF and PACF for Mokwa and Muwo

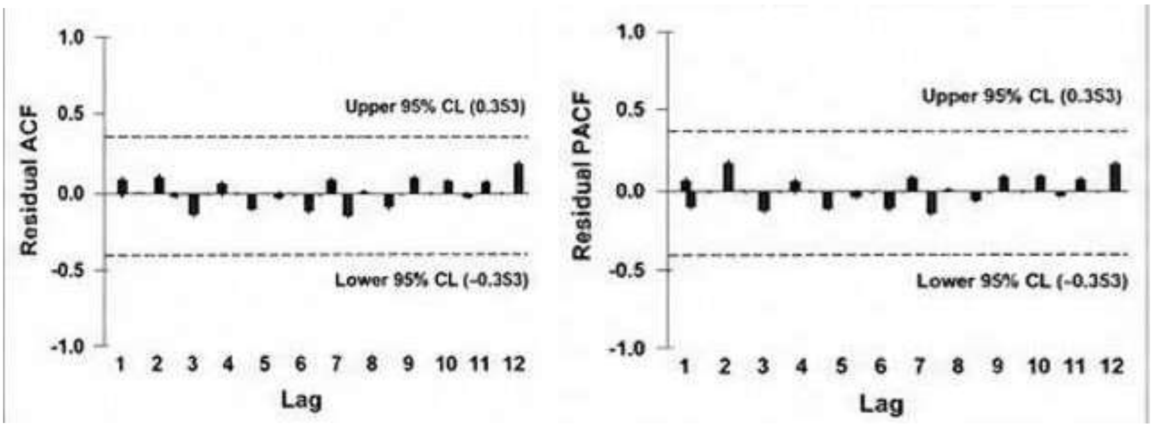

Figure 24: Rainfall ACF and PACF for Minna and Garatu

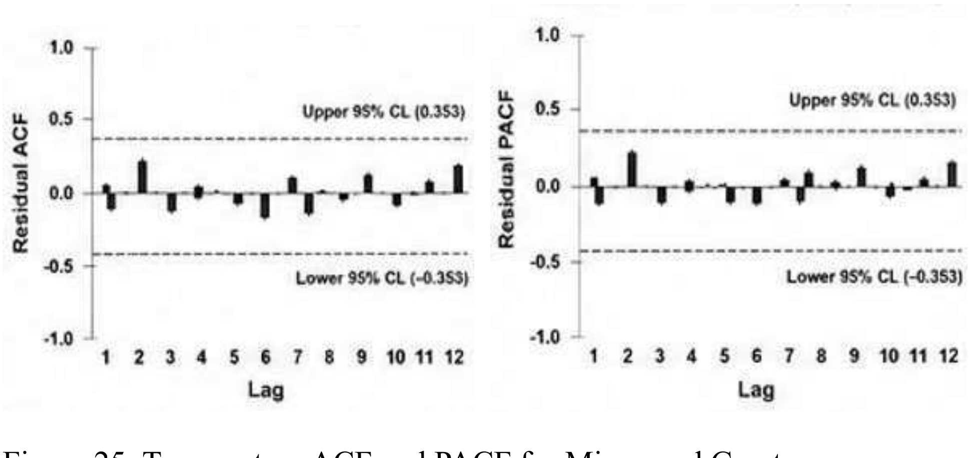

Figure 25: Temperature ACF and PACF for Minna and Garatu

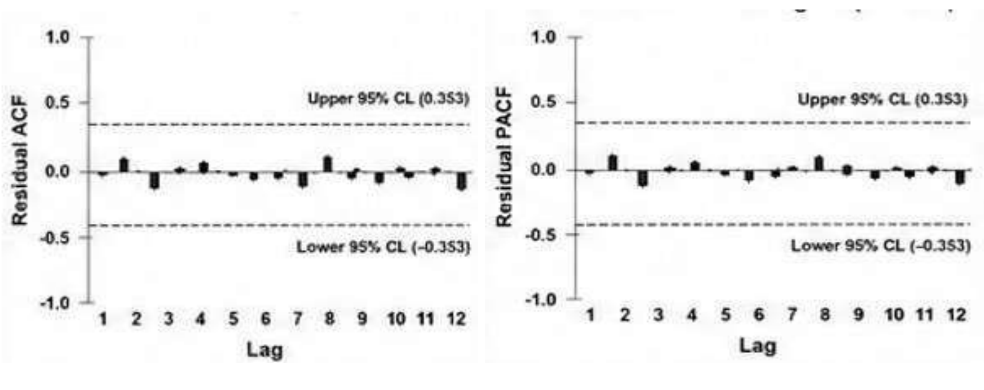

Figure 26: Rainfall ACF and PACF for Kontagora and Rafin Gora

ISSN No. 2454-6186 | DOI: 10.47772/IJRISS | Volume X Issue VII July 2026

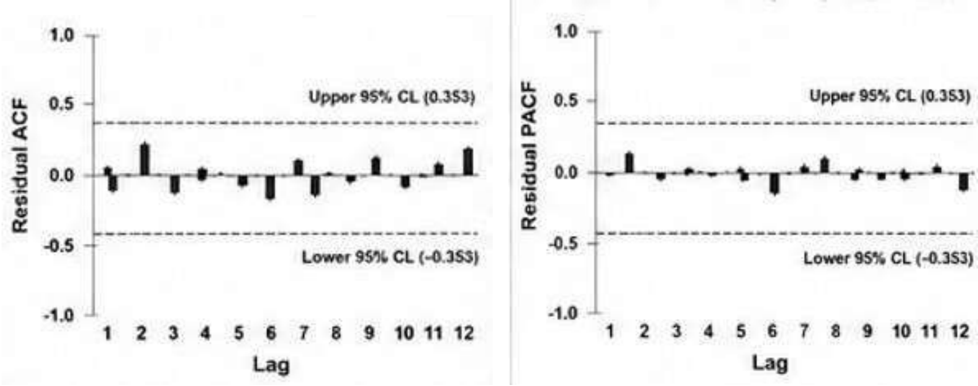

Figure 26: Temperature ACF and PACF for Kontagora

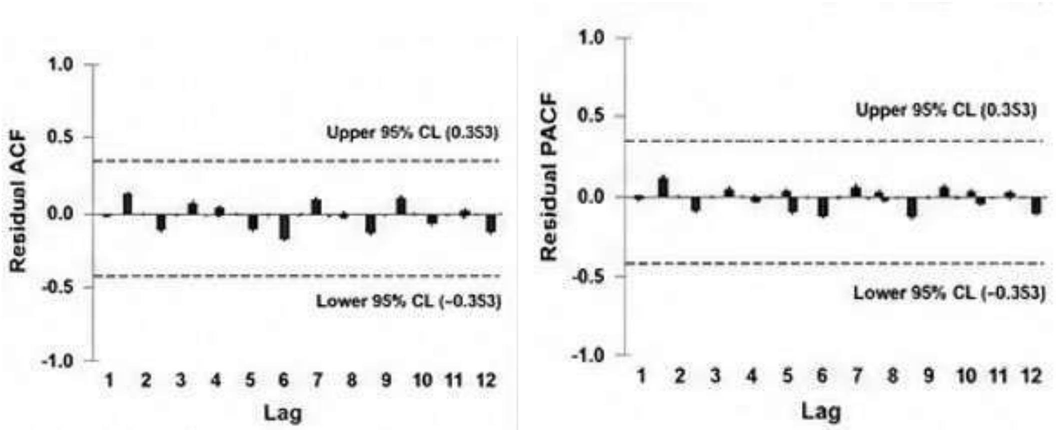

Figure 27: Temperature ACF and PACF for Rafin Gora

The Ljung–Box Q test results presented in Tables 23 and 24 indicate that the residuals of all fitted ARIMA models are statistically independent. For both rainfall and temperature models, the significance (p) values are greater than the 0.05 significance level, indicating that the null hypothesis of no residual autocorrelation cannot be rejected. Consequently, the residuals behave as white noise, confirming that the selected ARIMA models adequately captured the temporal dependence in the climatic series. This implies that the models are statistically adequate and suitable for forecasting annual rainfall and temperature across the selected settlements.

Table 23: Ljung–Box Q Test Results for Annual Rainfall Models

Location	**Variable**	**Selected ARIMA Model**	**Q Statistic**	**df**	**Sig. (p-value)**	**Decision**
Mokwa	Rainfall	ARIMA(1,2,1)	8.913	12	0.710	Residuals are white noise
Muwo	Rainfall	ARIMA(1,2,1)	8.913	12	0.710	Residuals are white noise
Minna	Rainfall	ARIMA(1,2,1)	9.521	12	0.657	Residuals are white noise
Garatu	Rainfall	ARIMA(1,2,1)	9.521	12	0.657	Residuals are white noise
Kontagora	Rainfall	ARIMA(1,2,1)	9.148	12	0.691	Residuals are white noise
Rafin	Rainfall	ARIMA(1,2,1)	9.148	1	0.691	Residuals are

ISSN No. 2454-6186 | DOI: 10.47772/IJRISS | Volume X Issue VII July 2026

Gora				2		white noise

Source: Author's Computation (2026).

Table 24: Ljung–Box Q Test Results for Annual Temperature Models

Location	Variable	Selected ARIMA Model	Q Statistic	df	Sig. (p-value)	Decision
Mokwa	Temperature	ARIMA(1,1,1)	8.264	12	0.764	Residuals are white noise
Muwo	Temperature	ARIMA(1,1,1)	8.264	12	0.764	Residuals are white noise
Minna	Temperature	ARIMA(1,1,1)	9.784	12	0.636	Residuals are white noise
Garatu	Temperature	ARIMA(1,1,1)	9.784	12	0.636	Residuals are white noise
Kontagora	Temperature	ARIMA(1,1,1)	10.426	12	0.578	Residuals are white noise
Rafin Gora	Temperature	ARIMA(1,1,1)	8.537	12	0.743	Residuals are white noise

Source: Author's Computation (2026).

Rainfall and Temperature Forecast

Figures 28 to 39 and Table 25 present the projected rainfall and temperature patterns across the six study settlements up to the year 2054. For Mokwa and Muwo, annual rainfall is projected to decline progressively from 942.58 mm in 2024 to 824.98 mm in 2034, 712.83 mm in 2044, and 600.69 mm by 2054. This continuous reduction is consistent with the negative Sen's Slope values obtained from the historical trend analysis and suggests a gradual decrease in future water availability within these settlements. In contrast, annual temperature is projected to increase steadily from 42.77°C in 2024 to 43.28°C in 2034, 43.79°C in 2044, and 44.30°C by 2054. The projected increase in temperature indicates persistent warming conditions, which may intensify heat stress and increase evapotranspiration rates, thereby compounding the effects of declining rainfall.

Comparable projections were observed for Minna and Garatu. Annual rainfall is forecast to decrease from 926.85 mm in 2024 to 805.42 mm in 2034, followed by further declines to 689.16 mm in 2044 and 574.93 mm by 2054. The magnitude of this projected decline is slightly greater than that observed in Mokwa and Muwo, reflecting the relatively larger negative Sen's Slope estimates recorded for these settlements. Conversely, temperature is projected to increase continuously from 43.08°C in 2024 to 43.66°C in 2034, 44.24°C in 2044, and 44.82°C by 2054. These projections suggest that Minna and Garatu may experience the most pronounced warming among all the study locations.

In contrast, Kontagora and Rafin Gora are projected to experience increasing rainfall conditions. Annual rainfall in both settlements is forecast to rise from 1886.28 mm in 2024 to 1932.40 mm in 2034, 1976.80 mm in 2044, and 2021.30 mm by 2054. This projected increase is consistent with the positive Sen's Slope values derived from the historical rainfall records. Temperature projections also indicate continued warming in both settlements, although the magnitude of increase differs considerably. In Kontagora, annual temperature is projected to increase from 41.49°C in 2024 to 43.14°C by 2054. Conversely, Rafin Gora is expected to experience only a slight increase in temperature, rising from 41.49°C to 41.76°C during the same period. These results suggest that future warming is likely to be considerably more pronounced in Kontagora than in Rafin Gora.

ISSN No. 2454-6186 | DOI: 10.47772/IJRISS | Volume X Issue VII July 2026

The simultaneous occurrence of declining rainfall and increasing temperature in Mokwa, Muwo, Minna, and Garatu may intensify drought conditions, reduce agricultural productivity, and place additional pressure on available water resources. Conversely, the projected increase in rainfall in Kontagora and Rafin Gora could potentially enhance water availability but may also elevate flood risks, particularly if future rainfall events become more intense. While the persistent warming projected across all settlements underscores the need for effective climate adaptation measures, sustainable land-use management, and resilient urban and rural development strategies. Such measures are essential for mitigating the potential impacts of future climate variability on agriculture, water resources, ecosystem sustainability, and human wellbeing within Niger State.

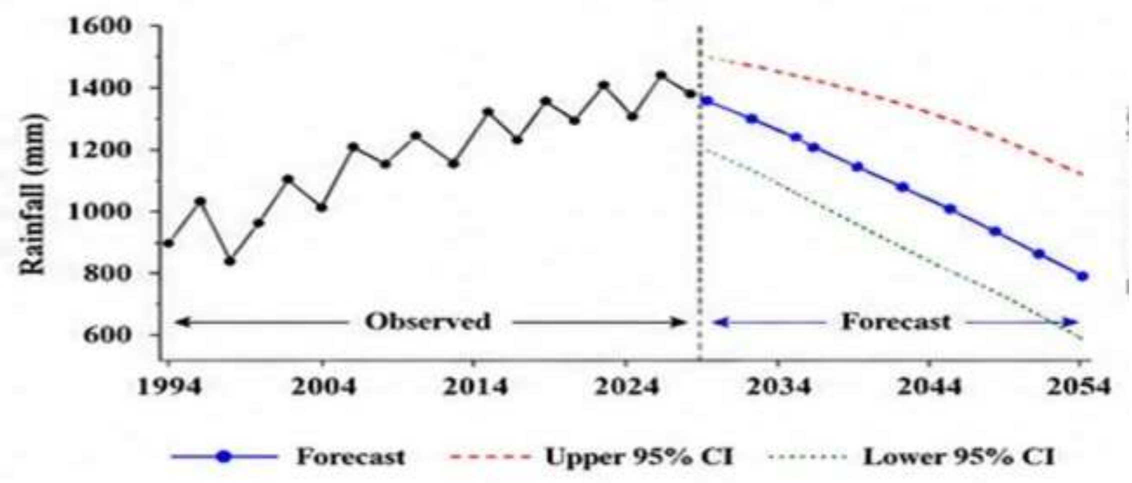

Figure 28: Observed and Forecast Annual Rainfall for Mokwa and Muwo (1994–2054)

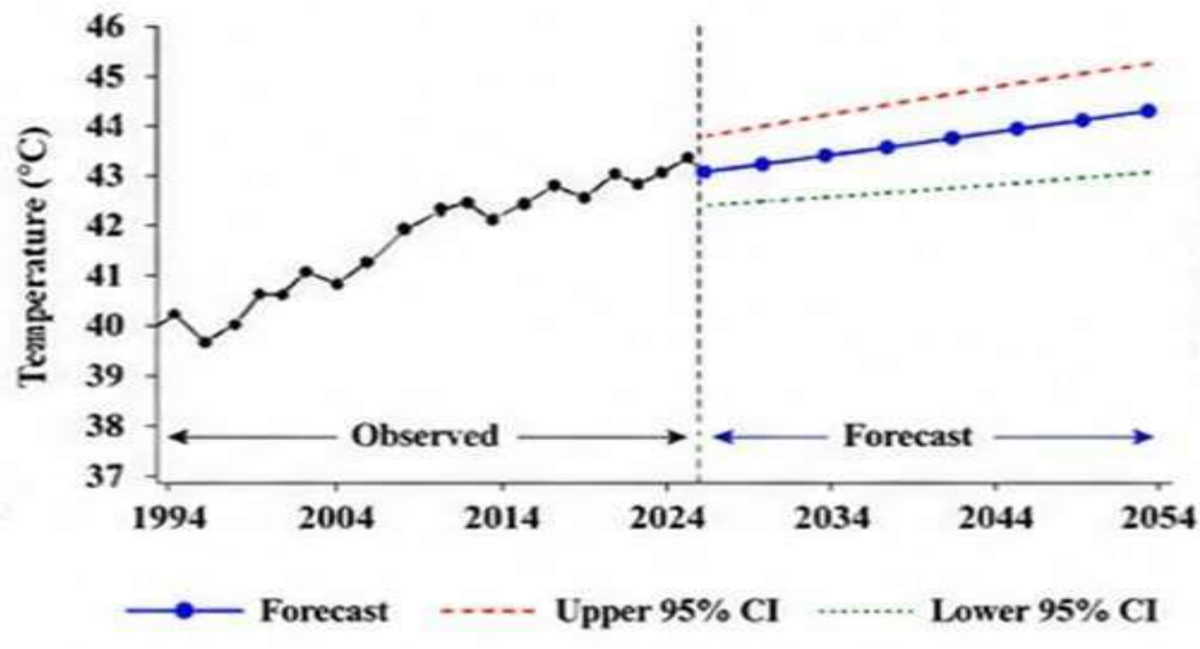

Figure 29: Observed and Forecast Annual Temperature for Mokwa and Muwo (1994–2054)

ISSN No. 2454-6186 | DOI: 10.47772/IJRISS | Volume X Issue VII July 2026

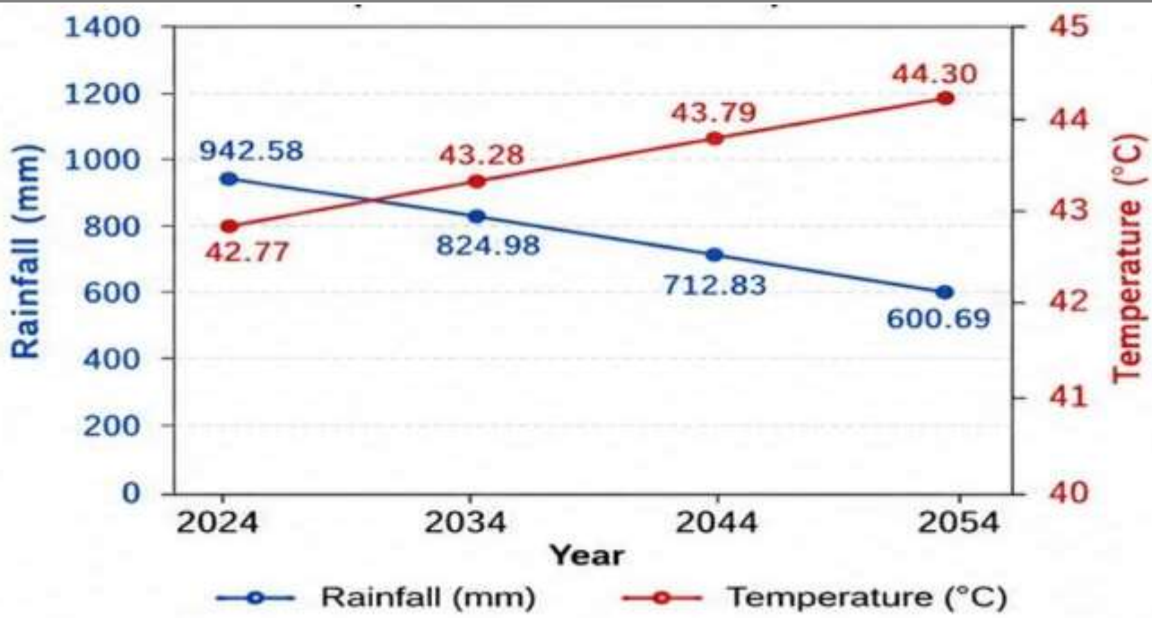

Figure 30: Observed and Forecast Annual Rainfall and Temperature for Mokwa and Muwo (2024 - 2054

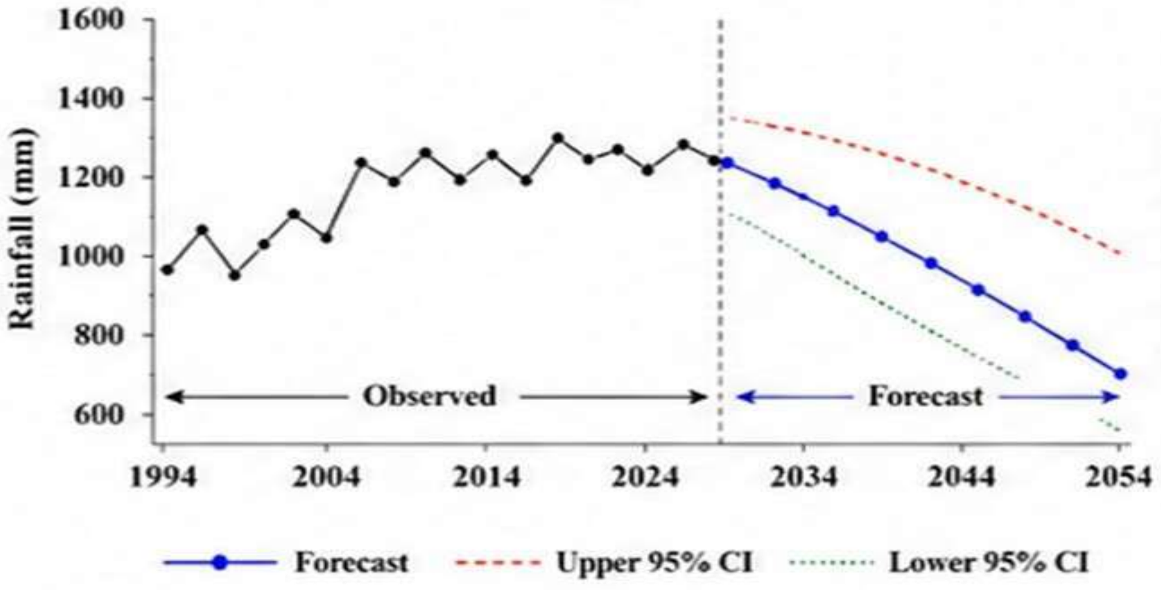

Figure 31: Observed and Forecast Annual Rainfall for Minna and Garatu (1994–2054)

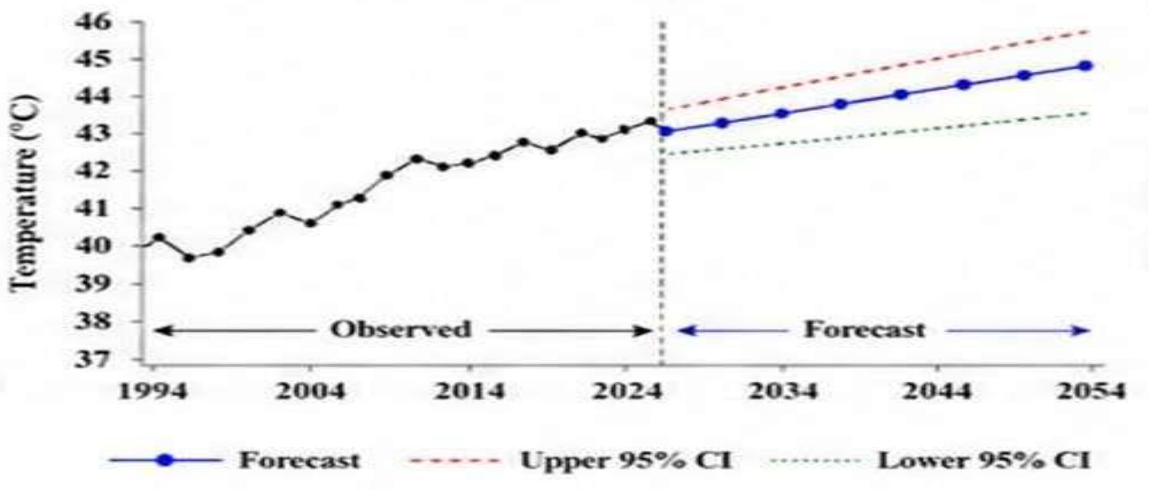

ISSN No. 2454-6186 | DOI: 10.47772/IJRISS | Volume X Issue VII July 2026

Figure 32: Observed and Forecast Annual Temperature for Minna and Garatu (1994–2054)

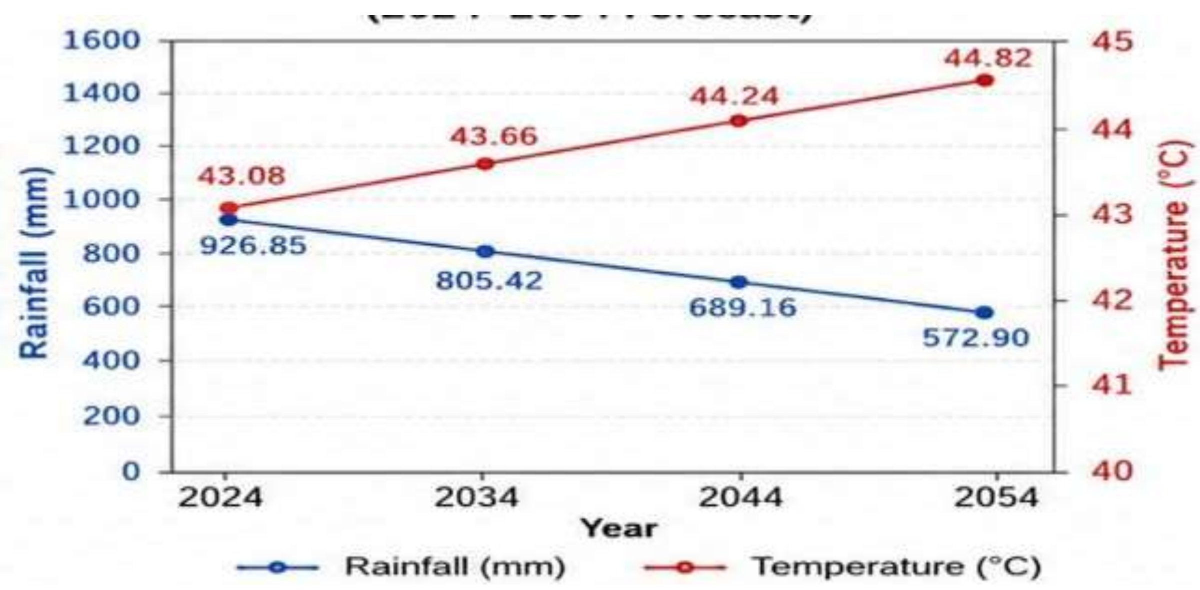

Figure 33: Observed and Forecast Annual Rainfall and temperature for Minna and Garatu (2024 – 2054)

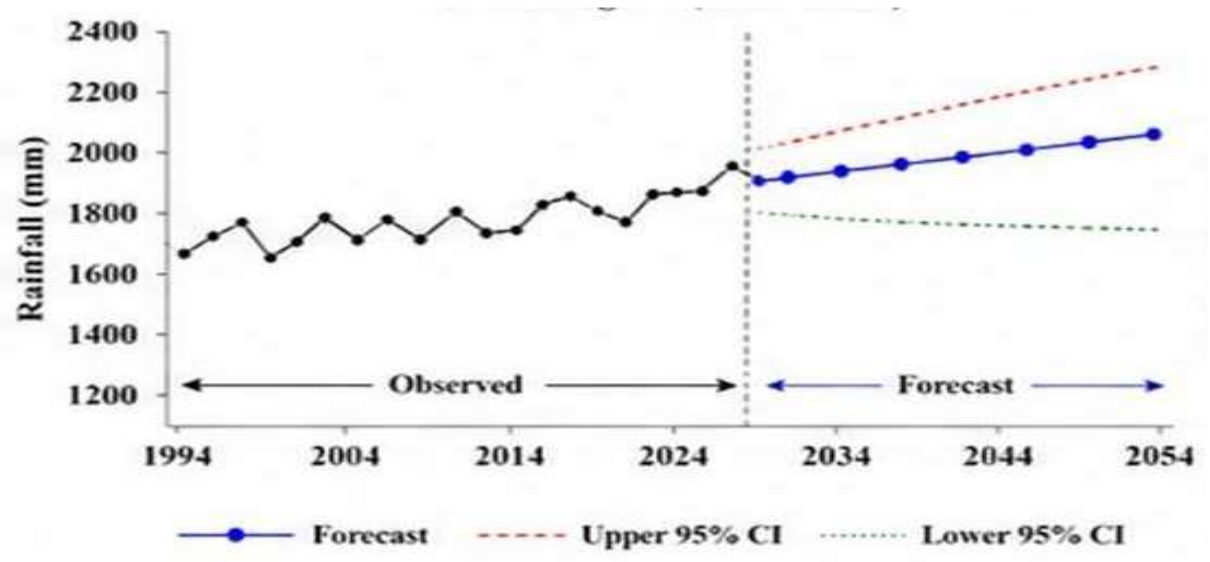

Figure 34: Observed and Forecast Annual Rainfall and Temperature for Kontagora Rafin Gora (1994–2054)

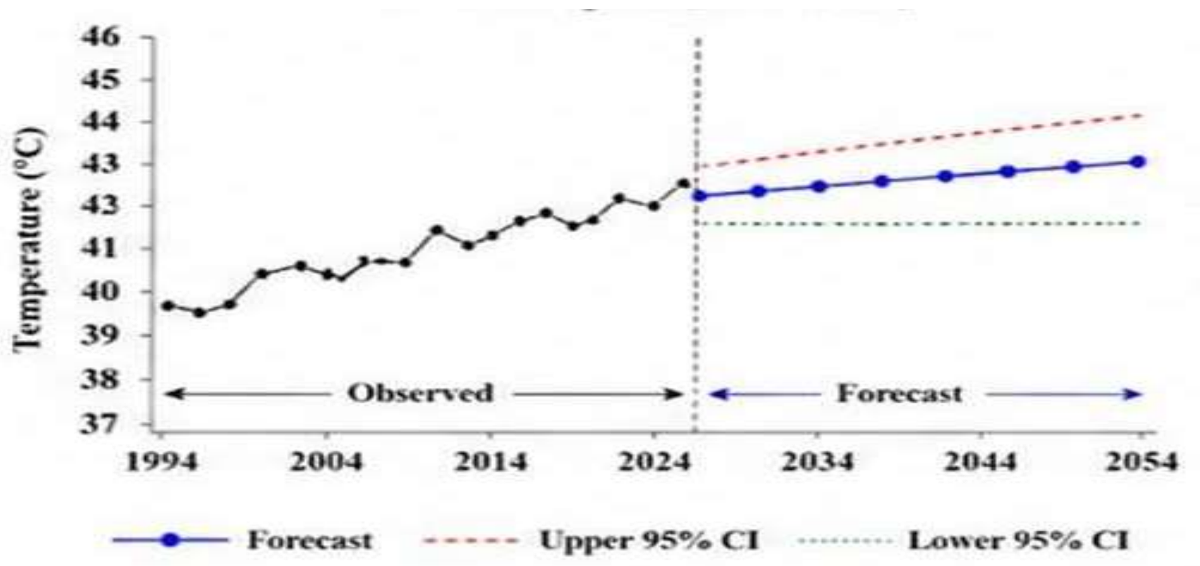

ISSN No. 2454-6186 | DOI: 10.47772/IJRISS | Volume X Issue VII July 2026

Figure 35: Observed and Forecast Annual Temperature for Kontagora (1994–2054)

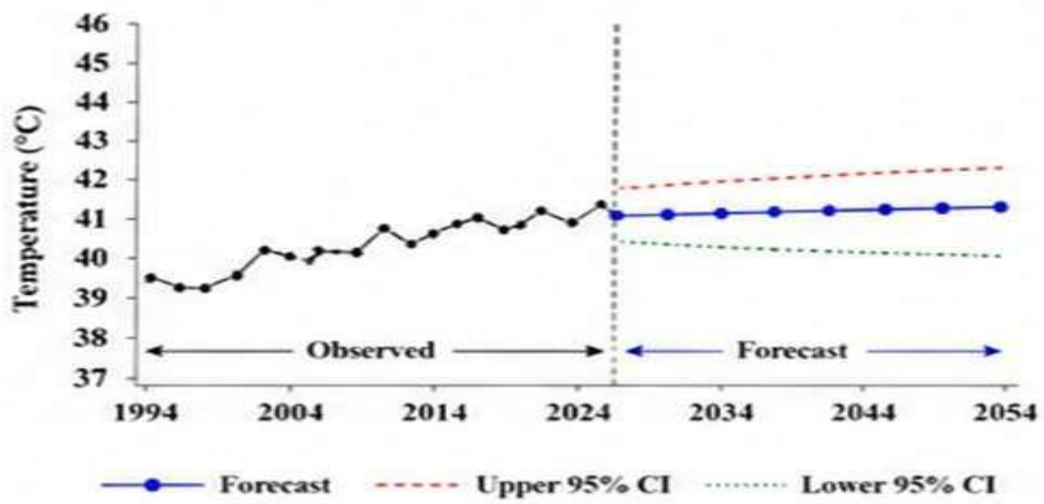

Figure 36: Observed and Forecast Annual Temperature for Rafin Gora (1994–2054)

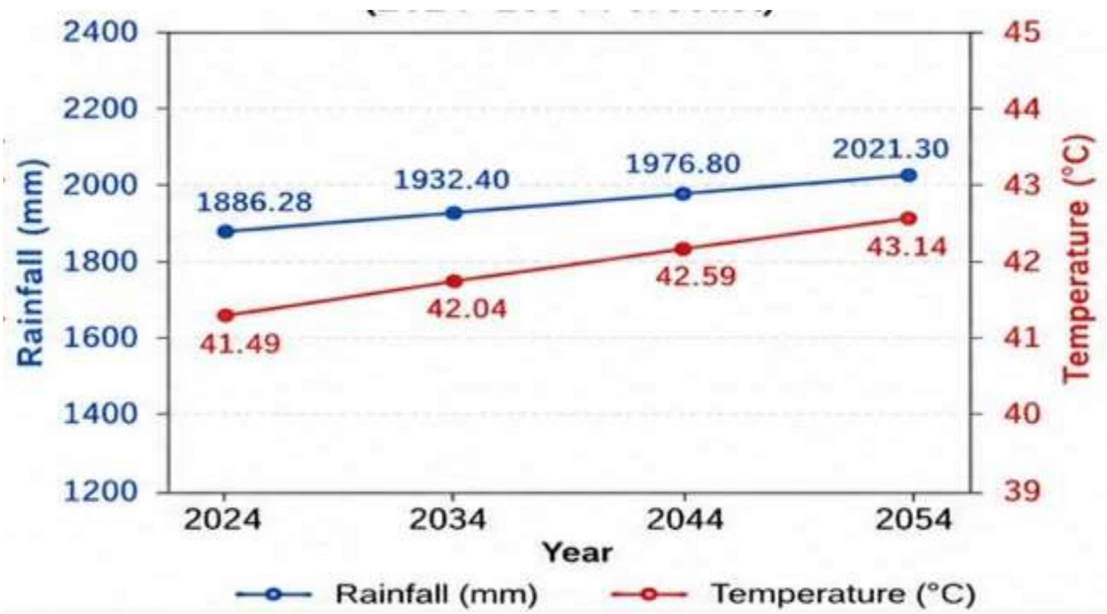

Figure 37: Observed and Forecast Annual Rainfall and Temperature Kontagora (1994–2054)

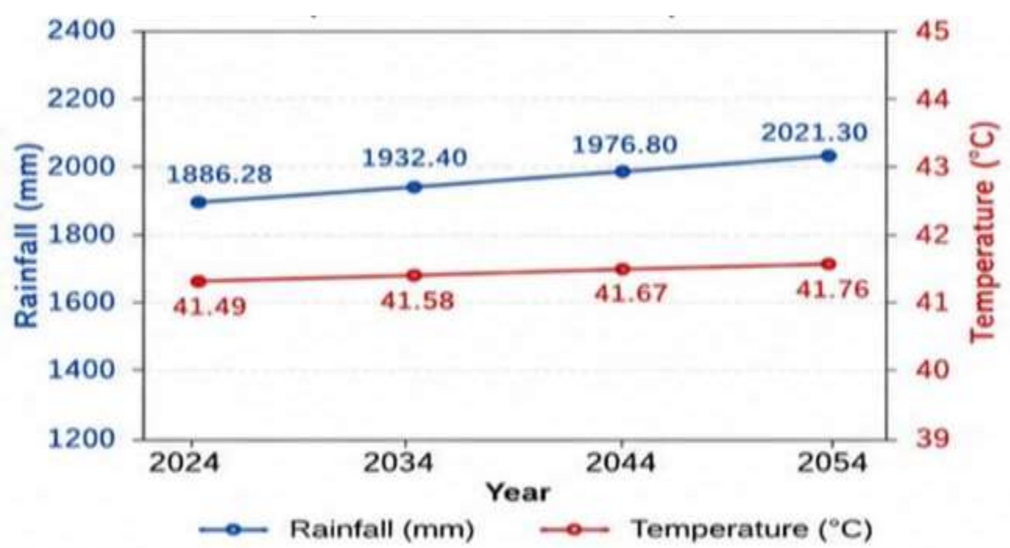

Figure 38: Observed and Forecast Annual Rainfall and Temperature for Rafin Gora (1994–2054)

ISSN No. 2454-6186 | DOI: 10.47772/IJRISS | Volume X Issue VII July 2026

Table 25: Analysis of Rainfall and Temperature Forecast Across Six Study Locations (2034, 2044 and 2054)

Location	**Variable**	**2024 Based Year**	**2034**	**2044**	**2054**	**Selected ARIMA Model**
Mokwa	Rainfall (mm)	942.58	824.98	712.83	600.69	ARIMA(1,2,1)
Mokwa	Temperature (°C)	42.77	43.28	43.79	44.30	ARIMA(1,1,1)
Muwo	Rainfall (mm)	942.58	824.98	712.83	600.69	ARIMA(1,2,1)
Muwo	Temperature (°C)	42.77	43.28	43.79	44.30	ARIMA(1,1,1)
Minna	Rainfall (mm)	926.85	805.42	689.16	574.93	ARIMA(1,2,1)
Minna	Temperature (°C)	43.08	43.66	44.24	44.82	ARIMA(1,1,1)
Garatu	Rainfall (mm)	926.85	805.42	689.16	574.93	ARIMA(1,2,1)
Garatu	Temperature (°C)	43.08	43.66	44.24	44.82	ARIMA(1,1,1)
Kontagora	Rainfall (mm)	1886.28	1932.40	1976.80	2021.30	ARIMA(1,2,1)
Kontagora	Temperature (°C)	41.49	42.04	42.59	43.14	ARIMA(1,1,1)
Rafin Gora	Rainfall (mm)	1886.28	1932.40	1976.80	2021.30	ARIMA(1,2,1)
Rafin Gora	Temperature (°C)	41.49	41.58	41.67	41.76	ARIMA(1,1,1)

Source: Author's Computation (2026).

DISCUSSION OF MAJOR FINDINGS

The analysis of climatic trends revealed contrasting responses between rainfall and temperature across the study settlements. Results from the Mann–Kendall trend test and Sen's Slope estimator demonstrated that rainfall exhibited both increasing and decreasing tendencies depending on geographical location, whereas temperature consistently increased across all six settlements. The most pronounced warming trends were observed in Minna and Garatu, while Rafin Gora recorded the weakest increase in temperature. These findings are consistent with the reports of the Intergovernmental Panel on Climate Change (2021, 2022), which identified increasing temperatures as one of the most evident manifestations of contemporary climate change, while emphasizing that rainfall patterns often exhibit substantial spatial variability due to regional atmospheric processes.

The observed warming trends also corroborate the findings of Adelekan et al. (2015) and IPCC (2023), who reported that urbanisation contributes to localised warming through increasing impervious surfaces and declining vegetation cover. Similarly, Iyeme et al. (2024) identified significant warming trends across Nigeria using the Mann–Kendall and Sen's Slope approaches. Furthermore, the declining rainfall trends recorded in some settlements align with earlier studies that documented increasing rainfall variability across West Africa (Nicholson, 2018). Consequently, the widespread warming observed across the study area reflects broader regional climate change patterns previously documented by IPCC (2023).

The ARIMA forecasting results further revealed persistent increases in temperature throughout the projection period across all study locations. In contrast, future rainfall projections indicated declining trends in Mokwa, Muwo, Minna, and Garatu, while Kontagora and Rafin Gora are projected to experience increasing rainfall conditions. These contrasting projections highlight the spatial complexity of precipitation dynamics within Niger State. The projected increases in temperature suggest that future climate variability may intensify, potentially increasing risks to agricultural productivity, water resources, biodiversity, and ecosystem stability. These findings are comparable to those reported by Adelekan et al. (2020), who observed that rapid urbanisation in Nigeria is associated with increasing thermal conditions and modifications in local climatic characteristics.

The projected continuation of warming, coupled with declining rainfall in some settlements, suggests increasing climate-related stress within Niger State. If appropriate adaptation and mitigation measures are not implemented, these changing climatic conditions may adversely affect agricultural production, water availability, ecosystem resilience, and overall socio-economic development within the state.

CONCLUSION

This study examined rainfall and temperature variability across selected urban and rural settlements in Niger State between 1994 and 2024 and projected future climatic conditions up to 2054. The findings revealed spatial variations in rainfall patterns, with declining trends observed in Mokwa, Muwo, Minna, and Garatu, while Kontagora and Rafin Gora exhibited increasing rainfall tendencies. In contrast, temperature showed a consistent increasing trend across all settlements, with urban centres generally experiencing stronger warming than rural areas. The future climate projections further indicate that these trends are likely to persist up to 2054. Rainfall is projected to continue decreasing in Mokwa, Muwo, Minna, and Garatu, whereas increasing rainfall conditions are expected in Kontagora and Rafin Gora. Similarly, temperature is forecast to rise continuously across all locations, suggesting intensified heat conditions and increasing climatic stress in the study area. These projections imply that the combined effects of rising temperatures and changing rainfall regimes may become more pronounced if current urbanisation and land-use transformation patterns continue. Therefore, the findings highlight the growing vulnerability of Niger State to future climate variability and underscore the necessity for proactive adaptation measures. Sustainable water-resource management, afforestation and ecosystem restoration programmes, climate-smart agricultural practices, and improved environmental and urban planning are therefore essential to enhance resilience and mitigate the adverse impacts of future climatic changes across both urban and rural settlements.

RECOMMENDATIONS

Based on the findings of this study, the following recommendations are made:

1. Integrate climate considerations into planning: Urban development policies should incorporate climate adaptation measures, including heat mitigation, sustainable drainage systems, and resilient infrastructure.

2. Improve climate monitoring: Meteorological monitoring networks should be strengthened to provide reliable long-term rainfall and temperature data for planning and research.

Suggestion for Further Studies

Based on the analysis and findings of this study, the following suggestions are made:

1. Future studies should incorporate higher temporal resolution climate data (monthly and seasonal datasets) to improve climate modelling accuracy.

2. Comparative studies between Niger State and states in Nigeria are also recommended to establish broader national climate patterns.

3. Future research may expand the study to include all local government areas of Niger State to provide a broader regional assessment.

REFERENCES

1. Adelekan, I. O., Johnson, C. A., Manda, M. Z., Matyas, D., Mberu, B., Parnell, S., Satterthwaite, D., & Vivekananda, J. (2015). Disaster risk and its reduction: An agenda for urban Africa. International Development Planning Review, 37(1), 33–43. https://doi.org/10.3828/idpr.2015.4
2. Adelekan, I. O., Johnson, C., Manda, M., Matyas, D., & Roberts, D. (2020). Climate change adaptation in Nigeria: A review of policy and practice. Climate and Development, 12(4), 295–307.
3. Agaj, T., Budka, A., Janicka, E., et al. (2024). Forecasting water level changes using ARIMA and ETS models for sustainable environmental management. Scientific Reports, 14, Article 22444.
4. Ayanlade, A., Radeny, M., Morton, J. F., & Muchaba, T. (2018). Rainfall variability and adaptation strategies in Nigeria. Climate Risk Management, 22, 45–59.
5. Box, G. E. P., & Jenkins, G. M. (1976). Time series analysis: Forecasting and control. Holden-Day.
6. Box, G. E. P., Jenkins, G. M., Reinsel, G. C., & Ljung, G. M. (2015). Time series analysis: Forecasting and control (5th ed.). Wiley.
7. Doblas-Reyes, F. J., García-Serrano, J., Lienert, F., Biescas, A. P., & Rodrigues, L. R. L. (2013). Seasonal climate predictability and forecasting: Status and prospects. Bulletin of the American Meteorological Society, 94(8), 1089–1100. https://doi.org/10.1175/BAMS-D-12-00027.1
8. Elneel, L., Zitouni, M. S., Mukhtar, H., & Al-Ahmad, H. (2024). Examining sea levels forecasting using autoregressive and Prophet models. Scientific Reports, 14, Article 14337.
9. Fan, C. (2025). Global temperature anomaly forecast: A comparative analysis of ARIMA and ETS models. Advances in Economics, Management and Political Sciences, 144, 70–76.
10. Field, C. B., Barros, V. R., Dokken, D. J., Mach, K. J., Mastrandrea, M. D., Bilir, T. E., Chatterjee, M., Ebi, K. L., Estrada, Y. O., Genova, R. C., Girma, B., Kissel, E. S., Levy, A. N., MacCracken, S., Mastrandrea, P. R., & White, L. L. (Eds.). (2014). Climate change 2014: Impacts, adaptation, and vulnerability. Part A: Global and sectoral aspects. Contribution of Working Group II to the Fifth Assessment Report of the Intergovernmental Panel on Climate Change. Cambridge University Press.
11. Food and Agriculture Organization of the United Nations. (2023). The state of food and agriculture 2023: Revealing the true cost of food to transform agrifood systems. FAO.
12. Gilbert, R. O. (1987). Statistical methods for environmental pollution monitoring. Van Nostrand Reinhold.
13. Haines, A., & Ebi, K. (2019). The imperative for climate action to protect health. New England Journal of Medicine, 380(3), 263–273. https://doi.org/10.1056/NEJMra1807873
14. Helsel, D. R., Hirsch, R. M., Ryberg, K. R., Archfield, S. A., & Gilroy, E. J. (2020). Statistical methods in water resources (Techniques and Methods, Book 4, Chapter A3). U.S. Geological Survey. https://doi.org/10.3133/tm4A3
15. Hyndman, R. J., & Athanasopoulos, G. (2021). Forecasting: Principles and practice (3rd ed.). OTexts.
16. Intergovernmental Panel on Climate Change. (2021). Climate change 2021: The physical science basis. Cambridge University Press.
17. Intergovernmental Panel on Climate Change. (2022). Climate change 2022: Impacts, adaptation and vulnerability. Cambridge University Press.
18. Intergovernmental Panel on Climate Change. (2023). Climate change 2023: Synthesis report. Intergovernmental Panel on Climate Change.
19. Intergovernmental Science-Policy Platform on Biodiversity and Ecosystem Services. (2023). Assessment report on biodiversity and ecosystem services. IPBES.
20. Iyeme, E. E., Ekah, U. J., Njok, A. O., Agbo, E. P., & Offorson, G. C. (2024). Trend analysis of climate change across Nigeria: A Mann–Kendall and Sen's approach. Archives of Current Research International, 24(11), 450–467.

21. Kendall, M. G. (1975). Rank correlation methods (4th ed.). Griffin.
22. Lobell, D. B., Schlenker, W., & Costa-Roberts, J. (2011). Climate trends and global crop production since 1980. Science, 333(6042), 616–620. https://doi.org/10.1126/science.1204531
23. Mann, H. B. (1945). Nonparametric tests against trend. Econometrica, 13(3), 245–259.
24. Masson-Delmotte, V., Zhai, P., Pirani, A., et al. (2021). Climate change 2021: The physical science basis. Cambridge University Press.
25. Merryfield, W. J., Lee, W. S., Boer, G. J., Dunstone, N., Doblas-Reyes, F. J., & Smith, D. M. (2020). Current and emerging developments in seasonal climate prediction. Bulletin of the American Meteorological Society, 101(7), E869–E896. https://doi.org/10.1175/BAMS-D-19-0138.1
26. National Bureau of Statistics. (2022). Population and urban growth statistics. Abuja, Nigeria.
27. Nicholson, S. E. (2018). The ITCZ and rainfall variability over West Africa. Climate Dynamics, 50, 3373–3391.
28. Niang, I., Ruppel, O. C., Abdrabo, M. A., et al. (2014). Africa. In C. B. Field et al. (Eds.), Climate change 2014: Impacts, adaptation, and vulnerability. Cambridge University Press.
29. Oguntunde, P. G., Lischeid, G., Abiodun, B. J., & Dietrich, O. (2020). Climate variability and temperature trends in Nigeria. Theoretical and Applied Climatology, 141, 105–120.
30. Oke, T. R. (1982). The energetic basis of the urban heat island. Quarterly Journal of the Royal Meteorological Society, 108(455), 1–24. https://doi.org/10.1002/qj.49710845502
31. Oyeniyi, A. S., Akinyemi, F. O., & Adewumi, T. O. (2025). Urban expansion and land surface temperature dynamics in medium-sized cities of southwestern Nigeria. Climate, 13(4), Article 68.
32. Parmesan, C., & Yohe, G. (2003). A globally coherent fingerprint of climate change impacts across natural systems. Nature, 421(6918), 37–42. https://doi.org/10.1038/nature01286
33. Sen, P. K. (1968). Estimates of the regression coefficient based on Kendall's tau. Journal of the American Statistical Association, 63(324), 1379–1389.
34. Şen, Z. (2024). Moving trend analysis methodology for hydro-meteorology time series dynamic assessment. Water Resources Management, 38, 4415–4429.
35. Smith, D. M., Eade, R., Dunstone, N. J., Fereday, D., Hermes, M., & Murphy, J. M. (2019). Robust skill in decadal climate predictions. Geophysical Research Letters, 46(10), 5449–5457. https://doi.org/10.1029/2019GL082559
36. Sultan, B., & Gaetani, M. (2016). Agriculture in West Africa in the twenty-first century: Climate change and impacts scenarios, and potential for adaptation. Frontiers in Plant Science, 7, Article 1262. https://doi.org/10.3389/fpls.2016.01262
37. Sylla, M. B., Nikiema, P. M., Gibba, P., Kebe, I., & Klutse, N. A. B. (2016). Climate change over West Africa. Current Climate Change Reports, 2, 193–205.
38. Trenberth, K. E., Fasullo, J. T., & Shepherd, T. G. (2014). Attribution of climate extreme events. Journal of Climate, 27(9), 3129–3144. https://doi.org/10.1175/JCLI-D-13-00500.1
39. United Nations Educational, Scientific and Cultural Organization. (2024). United Nations world water development report 2024: Water for prosperity and peace. UNESCO.
40. United Nations Environment Programme. (2024). Adaptation gap report 2024: Come hell and high water. UNEP.
41. Vörösmarty, C. J., McIntyre, P. B., Gessner, M. O., Dudgeon, D., Prusevich, A., Green, P., Glidden, S., Bunn, S. E., Sullivan, C. A., Reidy Liermann, C., & Davies, P. M. (2010). Global threats to human water security and river biodiversity. Nature, 467(7315), 555–561. https://doi.org/10.1038/nature09440
42. World Meteorological Organization. (2017). WMO guidelines on the calculation of climate normals (WMO-No. 1203). World Meteorological Organization.
43. World Meteorological Organization. (2017). Climate information and monitoring services. World Meteorological Organization.